

Characterizing Planetary Orbits and the Trajectories of Light

F.T. Hioe* and David Kuebel

Department of Physics, St. John Fisher College, Rochester, NY 14618

and

Department of Physics & Astronomy, University of Rochester, Rochester, NY 14627

December 16, 2018

Abstract

Exact analytic expressions for planetary orbits and light trajectories in the Schwarzschild geometry are presented. A new parameter space is used to characterize all possible planetary orbits. Different regions in this parameter space can be associated with different characteristics of the orbits. The boundaries for these regions are clearly defined. Observational data can be directly associated with points in the regions. A possible extension of these considerations with an additional parameter for the case of Kerr geometry is briefly discussed.

PACS numbers: 04.20.Jb, 02.90.+p

1 Introduction

Nearly a century after Einstein's theory of general relativity was found to correctly predict the precession of the planet Mercury around the sun and the deflection of light by the sun's gravitational field, the problem of understanding orbital trajectories around very massive objects still retains interest as it relates to current astrophysical topics [1] such as the study of gravitational waves. Among the numerous works on this subject, we should mention the classic publications of Whittaker [2], Hagihara [3] and Chandrasekhar [4] on the Schwarzschild geometry, and the more recent work of Levin and Perez-Giz [5] on the Schwarzschild and Kerr geometries.

In the work of Chandrasekhar and that of Hagihara, the orbits are classified into various types according to the roots of a certain cubic equation, while in the work of Levin and Perez-Giz, the orbits are classified topologically by a triplet of numbers that indicate the numbers of zooms, whirls and vertices. In the work of Levin and Perez-Giz, the orbits were obtained by numerically integrating the integrable equations. These authors used the planet's energy and angular momentum as the principal physical parameters, and made extensive use of an

effective potential for describing the Schwarzschild orbits, as most studies on the topics of general relativity do.

In this paper, we first present, in Section 2, three explicit analytic expressions for the orbits in the Schwarzschild geometry: one is for periodic orbits [6] (including a special case that we call asymptotic), and two are terminating orbits. The explicit analytic expressions that we derive not only describe the precise features of the orbits (periodic, precessing, non-periodic, terminating, etc.) but also clearly indicate two physical parameters which can be used to characterize these orbits. These two dimensionless parameters are specific combinations of the following physical quantities: the total energy and angular momentum of the planet, the masses of the massive object and the planet, and, of course, the universal gravitation constant G and the speed of light c . These two physical dimensionless parameters were first used by one of us in ref.6. We shall refer to these two quantities as the energy eccentricity parameter e and the gravitational field parameter s respectively (or simply as the energy parameter and the field parameter). They will be defined in Section 2. We will use neither the common convention of setting $G = c = 1$, nor the energy and angular momentum of the planet by themselves, as the physical parameters for characterizing the orbits. With the energy parameter ($0 \leq e \leq 1$) plotted on the horizontal axis and the field parameter ($0 \leq s \leq \infty$) plotted on the vertical axis, the parameter space for all possible orbits will be shown to be divisible into three sectors, which we call Regions I, II and II', that have clearly defined boundaries. Region I permits periodic and terminating orbits. Regions II and II' terminating orbits only.

In Section 3, we describe Region I for the orbits in greater detail. We first divide Region I by lines each of which represents orbits described by elliptic functions of the same modulus k . We then give a more physical division of Region I which consists of nearly horizontal lines each of which represents orbits that have the same precession angle $\Delta\phi$, and of bent vertical lines each of which represents orbits that have the same "true" eccentricity ε . The terminating orbits will be characterized by two parameters one of which is the angle at which the planet enters the center of the blackhole, and the other being the initial distance of the planet from the star or blackhole. In Sections 4 and 5, we describe Regions II and II' in which all orbits are terminating, and we again divide Region II by curves of constant modulus k each of which describes orbits with the same modulus. Regions II and II' are separated by the Schwarzschild horizon. Thus the grid of our "map" can be used to describe all possible orbits in the Schwarzschild geometry in their entirety. The observational data related to a planet's orbit about some giant star or blackhole can be directly identified with a point having certain coordinates (e, s) on our map, which can then be used for estimating the physical characteristics associated with the star or blackhole and that of the planet itself, assuming that the star or blackhole is not spinning very fast. For the Kerr geometry, another dimensionless quantity, which is clearly the ratio of the spin angular momentum per unit mass of the blackhole to the orbital angular momentum per unit mass of the planet, should enter into the consideration. In Section 6, we briefly discuss a possible extension of our results to the case involving a slowly spinning blackhole, at least to the first order

perturbation, by rescaling the physical parameters involved.

In Section 7, we study the deflection of light by the gravitational field of a very massive object. A single dimensionless parameter will be used to characterize the region. We show that here too, we should divide the region into three sectors, which we again call Regions I, II and II', and we present three analytic expressions for the trajectories of light applicable in these different regions. Region I has trajectories of light that get deflected, and Regions II and II' have trajectories of light that are absorbed by and terminate at the blackhole.

In Section 8, we give a summary of our results. Proofs of many interesting analytic relations among the parameters appearing in these studies are given in several appendices. Since our results presented in this paper cover gravitational fields of all ranges, from the weak field produced by the sun of our solar system, for example, to the very strong field produced by a blackhole, we want to avoid referring to the massive object that produces the gravitational field as a blackhole, and prefer to refer to it as the star or blackhole, and we shall refer to the object of a much smaller mass that orbits around it as the planet or the particle.

We have supplemented our many analytic results with numerous tables that present various physical quantities such as the minimum and maximum distances of the planet from the star and the angles of precession of the orbits that are calculated from our analytic expressions, as well as numerous figures that show various kinds of orbits of the planet and various kinds of deflection of light.

2 Analytic Expressions for the Orbits

We consider the Schwarzschild geometry, i.e. the static spherically symmetric gravitational field in the empty space surrounding some massive spherical object such as a star or a blackhole of mass M . The Schwarzschild metric for the empty spacetime outside a spherical body in the spherical coordinates r, θ, ϕ is [1]

$$dl^2 = c^2 \left(1 - \frac{\alpha}{r}\right) dt^2 - \left(1 - \frac{\alpha}{r}\right)^{-1} dr^2 - r^2 d\theta^2 - r^2 \sin^2 \theta d\phi^2 \quad (1)$$

where

$$\alpha = \frac{2GM}{c^2} \quad (2)$$

is known as the Schwarzschild radius, G is the universal gravitation constant, and c is the speed of light. If $[x^\mu] = (t, r, \theta, \phi)$, then the worldline $x^\mu(\tau)$, where τ is the proper time along the path, of a particle moving in the equatorial plane $\theta = \pi/2$, satisfies the equations [1]

$$\left(1 - \frac{\alpha}{r}\right) \dot{t} = \kappa, \quad (3)$$

$$c^2 \left(1 - \frac{\alpha}{r}\right) \dot{t}^2 - \left(1 - \frac{\alpha}{r}\right)^{-1} \dot{r}^2 - r^2 \dot{\phi}^2 = c^2, \quad (4)$$

$$r^2 \dot{\phi} = h, \quad (5)$$

where the derivative $\dot{}$ represents $d/d\tau$. The constant h is identified as the angular momentum per unit mass of the planet, and the constant κ is identified to be

$$\kappa = \frac{E}{m_0 c^2},$$

where E is the total energy of the planet in its orbit and m_0 is the rest mass of the planet at $r = \infty$. Substituting eqs.(3) and (5) into (4) gives the 'combined' energy equation [1]

$$\dot{r}^2 + \frac{h^2}{r^2} \left(1 - \frac{\alpha}{r}\right) - \frac{c^2 \alpha}{r} = c^2(\kappa^2 - 1). \quad (6)$$

Substituting $dr/d\tau = (dr/d\phi)(d\phi/d\tau) = (h/r^2)(dr/d\phi)$ into the combined energy equation gives the differential equation for the orbit of the planet

$$\left(\frac{du}{d\phi}\right)^2 = \alpha u^3 - u^2 + Bu + C \quad (7)$$

where $u = 1/r$, $B = 2GM/h^2$, $C = c^2(\kappa^2 - 1)/h^2$. Following Whittaker [2], it is convenient to change variable from u to a dimensionless quantity U defined by

$$U = \frac{1}{4} \left(\frac{\alpha}{r} - \frac{1}{3}\right) = \frac{1}{4} \left(\alpha u - \frac{1}{3}\right), \quad (8)$$

or $u = 4U/\alpha + 1/(3\alpha)$ so that eq.(7) becomes

$$\left(\frac{dU}{d\phi}\right)^2 = 4U^3 - g_2 U - g_3 \quad (9)$$

where

$$\begin{aligned} g_2 &= \frac{1}{12} - s^2 \\ g_3 &= \frac{1}{216} - \frac{1}{12}s^2 + \frac{1}{4}(1 - e^2)s^4, \end{aligned} \quad (10)$$

and where

$$e = \left[1 + \frac{h^2 c^2 (\kappa^2 - 1)}{(GM)^2}\right]^{1/2} \quad (11)$$

and

$$s = \frac{GM}{hc}. \quad (12)$$

The two dimensionless parameters e and s , which are defined by the two above equations and which we call the energy and field parameters respectively, will be the principal parameters we shall use for characterizing the orbit of a planet. It will be noted that the constant $c^2(\kappa^2 - 1)$ which is < 0 for a bound orbit, can be identified with $2E_0/m$ in the Newtonian limit, where E_0 is the sum of the kinetic and potential energies and is < 0 for a bound orbit, and m is the mass of the planet (which approaches m_0), and that

$$e \simeq \left[1 + \frac{2E_0 h^2}{m(GM)^2} \right]^{1/2} \quad (13)$$

is the "eccentricity" of the orbit. Also, in the small s limit, the orbit equation can be shown to be given by

$$\frac{1}{r} \simeq \frac{GM}{h^2} [1 - e \cos(1 - \delta)\phi], \quad (14)$$

where $\delta \simeq 3(GM)^2/(hc)^2$. Thus r assumes the same value when ϕ increases to $\phi + 2\pi/(1 - \delta)$. Comparing this with the increase of ϕ from ϕ to $\phi + 2\pi$, the ellipse will rotate about the focus by an amount which is the angle of precession

$$\Delta\phi \simeq \frac{2\pi}{1 - \delta} - 2\pi \simeq 2\pi\delta = \frac{6\pi(GM)^2}{h^2 c^2}. \quad (15)$$

This is the well known approximate expression for the precession angle for the case of very small s . The limiting case for $\delta = 0$ is the well known orbit equation in Newtonian mechanics. We should note that while the limit $s = 0$ (and thus $\delta = 0$) cannot be strictly correct in principle so long as $M \neq 0$, this limit can be used for many practical cases with great accuracy as evidenced by the predictions of Newtonian mechanics. A special case of these Newtonian orbits is the circular orbit of radius $r = h^2/GM$ for $e = 0$.

We now derive the exact analytic solutions of eq.(9) and classify the three possible solutions from a purely mathematical viewpoint, and we shall consider their physical interpretations in the next section. We first define the discriminant Δ of the cubic equation

$$4U^3 - g_2U - g_3 = 0 \quad (16)$$

by

$$\Delta = 27g_3^2 - g_2^3. \quad (17)$$

The three roots of the cubic equation (16) are all real for the case $\Delta \leq 0$. We call the three roots e_1, e_2, e_3 and arrange them so that $e_1 > e_2 > e_3$; the special cases when two of the roots are equal will be considered also. For the case $\Delta > 0$, the cubic equation (16) has one real root and two roots that are complex conjugates. The analytic solutions of eq.(9) that we shall present will give the distance r of the planet from the star or blackhole in terms of the Jacobian elliptic functions that have the polar angle ϕ in their argument and

that are associated with a modulus k that will be defined. Instead of writing r , we use the dimensionless distance q measured in units of the Schwarzschild radius α and defined by

$$q \equiv \frac{r}{\alpha} \equiv \frac{1}{\alpha u}. \quad (18)$$

The dimensionless distance q is related to U of eq.(8) by

$$\frac{1}{q} = \frac{1}{3} + 4U. \quad (19)$$

We now give the three analytic solutions of eq.(9) in the following.

Solution (A1) For $\Delta \leq 0$, $e_1 > e_2 \geq U > e_3$.

Writing the right-hand side of eq.(9) as $4(e_1 - U)(e_2 - U)(U - e_3)$, eq.(9) can be integrated with ϕ expressed in terms of the inverse Jacobian sn function [7]. After a little algebra and some rearrangement, the equation for the orbit is found to be

$$\begin{aligned} \frac{1}{q} &= \frac{1}{3} + 4e_3 + 4(e_2 - e_3)sn^2(\gamma\phi, k) \\ &= \frac{1}{3} + 4e_3 + 4(e_2 - e_3)\frac{1 - cn(2\gamma\phi, k)}{1 + dn(2\gamma\phi, k)}, \end{aligned} \quad (20)$$

where the point at $\phi = 0$ has been chosen to give $U = e_3$. The constant γ appearing in the argument, and the modulus k , of the Jacobian elliptic functions are given in terms of the three roots of the cubic equation (16) by

$$\gamma = (e_1 - e_3)^{1/2}, \quad (21)$$

$$k^2 = \frac{e_2 - e_3}{e_1 - e_3}. \quad (22)$$

where e_1, e_2, e_3 are given by

$$\begin{aligned} e_1 &= 2 \left(\frac{g_2}{12}\right)^{1/2} \cos\left(\frac{\theta}{3}\right), \\ e_2 &= 2 \left(\frac{g_2}{12}\right)^{1/2} \cos\left(\frac{\theta}{3} + \frac{4\pi}{3}\right), \\ e_3 &= 2 \left(\frac{g_2}{12}\right)^{1/2} \cos\left(\frac{\theta}{3} + \frac{2\pi}{3}\right), \end{aligned} \quad (23)$$

and where

$$\cos\theta = g_3 \left(\frac{27}{g_2^3}\right)^{1/2}. \quad (24)$$

Equation (20) was first given in ref.6 using a slightly different approach that was initiated by Whittaker [2]. In addition, eq.(20) was shown to reduce to eq.(14) for the case of very small s which in turn gave the known approximate precession angle given by eq.(15). The modulus k of the elliptic functions has a range $0 \leq k^2 \leq 1$. Since the elliptic functions sn , cn and dn are all periodic functions of ϕ for $0 \leq k^2 < 1$, we shall call this solution for the orbit the periodic solution. For the special case of $k^2 = 1$, since $sn(\gamma\phi, 1) = \tanh(\gamma\phi)$, $cn(\gamma\phi, 1) = dn(\gamma\phi, 1) = \text{sech}(\gamma\phi)$, the solution is no longer periodic, and we shall refer to it as the asymptotic periodic solution.

The period of $cn(2\gamma\phi, k)$ is $4K(k)$, and the period of $dn(2\gamma\phi, k)$ and of $sn^2(\gamma\phi, k)$ is $2K(k)$, where $K(k)$ is the complete elliptic integral of the first kind [7]. For $k = 0$, $sn(x, 0) = \sin x$, $cn(x, 0) = \cos x$, $dn(x, 0) = 1$. As k^2 increases from 0 to 1, $K(k)$ increases from $\pi/2$ to ∞ . The distance r of the planet from the center of the star or blackhole assumes the same value when its polar angle ϕ increases from ϕ to $\phi + 4K/(2\gamma) = \phi + 2K/\gamma$. Comparing this with the increase of ϕ from ϕ to $\phi + 2\pi$ in one revolution, the perihelion (or the aphelion) will rotate by an amount

$$\Delta\phi = \frac{2K(k)}{\gamma} - 2\pi, \quad (25)$$

which is the exact expression for the precession angle. For k^2 close to the value 1, the planet can make many revolutions around the star or blackhole before assuming a distance equal to its initial distance. Thus if n is the largest integer for which $2K(k)/\gamma$ is equal to or greater than $2n\pi$, the angle of precession should be more appropriately defined as $2K(k)/\gamma - 2n\pi$. For the sake of consistency, however, we shall stick to the definition given by eq.(25).

For the case of very small s and to the order of s^2 , it was shown in ref.6 that $\gamma \simeq [1 - (3 - e)s^2]/2$, $k^2 \simeq 4es^2$, $K(k) \simeq \pi(1 + es^2)/2$, and substituting these into eq.(25) gives the well known approximate result given by eq.(15).

For these periodic orbits, we note that the maximum distance r_{\max} (the aphelion) of the planet from the star or blackhole and the minimum distance r_{\min} (the perihelion) of the planet from the star or blackhole, or their corresponding dimensionless forms q_{\max} ($= r_{\max}/\alpha$) and q_{\min} ($= r_{\min}/\alpha$), are obtained from eq.(20) when $\gamma\phi = 0$ and when $\gamma\phi = K(k)$ respectively, and they are given by

$$\frac{1}{q_{\max}} = \frac{1}{3} + 4e_3, \quad (26)$$

and

$$\frac{1}{q_{\min}} = \frac{1}{3} + 4e_2, \quad (27)$$

where e_2 and e_3 are determined from eqs.(23), (24) and (10) in terms of e and s .

Although we call the orbits given by this solution for $0 \leq k^2 < 1$ periodic, they are not necessarily closed orbits. It is seen from the precession discussed

above that for $\Delta\phi = f\pi$, unless f is a rational number, the orbit will not close and it is not strictly a closed periodic orbit. However, for all practical purposes, any irrational number when truncated becomes a rational number, and thus the orbit will be closed. The distinction of closed and non-closed orbits depending on whether f is rational or irrational is of course of profound theoretical interest [5].

For a general periodic orbit that precesses, the general or true eccentricity ε of the orbit is defined by

$$\varepsilon \equiv \frac{r_{\max} - r_{\min}}{r_{\max} + r_{\min}} = \frac{q_{\max} - q_{\min}}{q_{\max} + q_{\min}}, \quad (28)$$

where q_{\max} and q_{\min} are given by eqs.(26) and (27).

We shall show in the following section that the true eccentricity ε is in general not equal to the energy eccentricity parameter e defined by eq.(11), but that $\varepsilon \rightarrow e$ in the limit of $s \rightarrow 0$, i.e. in the Newtonian limit. For the special case of $\varepsilon = 1$ however, we shall show that it coincides with the special case of $e = 1$ for all applicable values of s , and that it signifies an unbounded orbit.

We now proceed to present the second solution.

Solution (A2) For $\Delta \leq 0$, $U > e_1 > e_2 > e_3$.

We write the right-hand side of eq.(9) as $4(U - e_1)(U - e_2)(U - e_3)$ and eq.(9) can be integrated with ϕ expressed in term of the inverse Jacobian sn function [7]. The equation for the orbit is found to be

$$\frac{1}{q} = \frac{1}{3} + 4 \frac{e_1 - e_2 sn^2(\gamma\phi, k)}{cn^2(\gamma\phi, k)}, \quad (29)$$

where γ , k , e_1 , e_2 and e_3 are given by eqs.(21)-(24) as in the first solution. This solution gives a terminating orbit. The point at $\phi = 0$ has been chosen to be given by

$$\frac{1}{q_1} = \frac{1}{3} + 4e_1. \quad (30)$$

The planet, starting from the polar angle $\phi = 0$ at a distance q_1 from the blackhole, plunges into the center of the blackhole when its polar angle ϕ_1 is given by $cn(\gamma\phi_1, k) = 0$, i.e. when

$$\phi_1 = \frac{K(k)}{\gamma},$$

where γ and k are given by eqs.(21) and (22).

The region of (e, s) where orbits given by solutions A1 and A2 are applicable will be called Region I, and it will be described in greater detail in Section 3. Thus each point (e, s) of parameter space in Region I represents two distinct orbits, one periodic and one terminating. At the same coordinate point, the characteristic quantities that describe the two distinct orbits are related. For

example, by noting $e_1 + e_2 + e_3 = 0$ and from eqs.(26) and (27), q_1 can be expressed as

$$\frac{1}{q_1} = 1 - \left(\frac{1}{q_{\min}} + \frac{1}{q_{\max}} \right), \quad (31)$$

where q_{\min} and q_{\max} are the minimum and maximum distances for the periodic orbit at the same coordinate points (e, s) . It will be noted that q_1 is less than q_{\min} , i.e. for the terminating orbit the planet is assumed initially to be closer to the blackhole than the q_{\min} for the associated periodic orbit, except at $k^2 = 1$ where $q_1 = q_{\min}$ and the planet has a circular instead of a terminating orbit that will be explained later.

We note that the terminating orbit equation (29) presented has no singularity at the Schwarzschild horizon $q = 1$, because, as is well known, $q = 1$ is a coordinate singularity and not a physical singularity. The orbit obtained from continuing ϕ beyond the value $\phi_1 = K(k)/\gamma$ may become interesting if the concept of "whitehole" turns out to be of physical relevance.

For now, the orbits in Region I are characterized mathematically by $\Delta \leq 0$.

We now present the third solution.

Solution (B) For $\Delta > 0$.

Define

$$\begin{aligned} A &= \frac{1}{2} \left(g_3 + \sqrt{\frac{\Delta}{27}} \right)^{1/3}, \\ B &= \frac{1}{2} \left(g_3 - \sqrt{\frac{\Delta}{27}} \right)^{1/3}, \end{aligned} \quad (32)$$

where g_3 and Δ are defined by eqs.(10) and (17). The real root of the cubic equation (16) is given by

$$a = A + B \quad (33)$$

and the two complex conjugate roots b and \bar{b} are $-(A+B)/2 \pm (A-B)\sqrt{3}i/2$. We further define

$$\gamma = [3(A^2 + AB + B^2)]^{1/4} \quad (34)$$

and

$$k^2 = \frac{1}{2} - \frac{3(A+B)}{4\sqrt{3(A^2 + AB + B^2)}} = \frac{1}{2} - \frac{3a}{4\gamma^2}. \quad (35)$$

Writing the right-hand side of eq.(9), with $U \geq a$, as $4(U-a)(U-b)(U-\bar{b})$, eq.(9) can be integrated with ϕ expressed in terms of the inverse Jacobian cn function [7]. We find the equation for the orbit to be

$$\frac{1}{q} = \frac{1}{3} + 4 \frac{\gamma^2 + a - (\gamma^2 - a)cn(2\gamma\phi, k)}{1 + cn(2\gamma\phi, k)}. \quad (36)$$

This is a terminating orbit. The initial distance q_2 of the planet at $\phi = 0$ has been chosen to be given by

$$\frac{1}{q_2} = \frac{1}{3} + 4a. \quad (37)$$

It plunges into the center of the blackhole when its polar angle $\phi = \phi_2$ is given by

$$\phi_2 = \frac{K(k)}{\gamma},$$

where γ and k are given by eqs.(34) and (35). Again, we note that the orbit equation (36) has no singularity at $q = 1$.

The region of (e, s) where orbits given by eq.(36) are applicable will be divided into two sectors called Regions II and II', the boundary between which will be defined later. They have terminating orbits only. For now, the orbits in Regions II and II' are characterized mathematically by $\Delta > 0$.

As for the initial points of the orbits discussed above, by comparing eq.(19) with the orbit equations (20), (29) and (36), and with eqs.(26), (30) and (37), we already noted that our choice of $\phi = 0$ in our orbit equations is such that it gives $U = e_3, e_1$, and a respectively that in turn give $q = q_{\max}, q_1$, and q_2 as the initial distances of the planet from the star or blackhole. We then note from eq.(9) that $dU/d\phi = 0$ and hence $dr/d\phi = 0$ for the planet at these initial points of the trajectories, i.e. the trajectory or more precisely the tangent to the trajectory at $\phi = 0$ is perpendicular to the line joining the planet to the star or blackhole. All this will be seen in the figures presented later, and all our references to the initial position of the planet from here onward assume that the trajectory (as ϕ increases from 0) of the planet at its initial position is perpendicular to the line joining the planet to the star or blackhole.

3 Region I

Consider the orbits expressed by eqs.(20) and (29) given by solutions A1 and A2 and characterized mathematically by $\Delta \leq 0$. We call the region covered by the associated range of values for (e, s) Region I.

To gain a preliminary perspective, consider the earth (as the planet) and the sun (as the star) in our solar system. Substituting the mass of the sun $M = M_S = 1.99 \times 10^{30}kg$ and the angular momentum of the earth per unit mass of the earth $h = 4.48 \times 10^{15}m^2/s$, we find $s = 0.983 \times 10^{-4}$. The energy eccentricity parameter e , which is equal to the true eccentricity ε of the earth's orbit for such a very small s value, is known to be about 0.017. The approximate relation $k^2 \simeq 4es^2$ gives the squared modulus of the elliptic functions that describe the earth's orbit to be $k^2 = 0.657 \times 10^{-9}$. We see that for the planetary system that

is familiar to us, the values of s and k^2 are very small indeed. We may also note that the Schwarzschild radius $\alpha = 2GM_S/c^2 \simeq 3 \text{ km}$ would be well inside the sun which has a radius of $6.4 \times 10^3 \text{ km}$. The earth's dimensionless distance is $q \simeq 5 \times 10^7$ from the sun's center. For this value of s , with $q_{\min} \simeq q_{\max} \simeq 5 \times 10^7$, the orbit given by eq.(29) from solution A2 would require the initial position q_1 of a planet to be $\simeq 1$ according to eq.(31), i.e. the planet would have to be at a distance equal to the Schwarzschild radius from the center of the sun for it to have a terminating orbit which plunges to the center of the sun. Therefore the terminating orbit given by eq.(29) is inapplicable for our solar system. The periodic orbits, on the other hand, are perfectly valid.

However, for cases when the massive object is a gigantic mass concentrated in a small radius such as a blackhole, all the possibilities presented here may arise. As the field parameter s increases from 0, the modulus k of the elliptic functions that describe the planet's orbits also increases. From eqs.(21)-(24), it is seen that several steps are needed to relate k^2 to e and s . In Appendix A, we show that a direct relationship between k^2 and e and s can be established, and it is given by

$$\begin{aligned} \frac{1 - 18s^2 + 54(1 - e^2)s^4}{(1 - 12s^2)^{3/2}} &= \frac{(2 - k^2)(1 + k^2)(1 - 2k^2)}{2(1 - k^2 + k^4)^{3/2}} & (38) \\ &= \cos \theta. & (39) \end{aligned}$$

The $\cos \theta$ of eq.(39) is the same $\cos \theta$ that appears in eq.(24), and, in particular, it is equal to 1, 0, -1 for $k^2 = 0, 1/2, 1$ respectively.

The curve represented by $k^2 = 1$, after setting $\cos \theta = -1$ in eq.(39), can be readily shown to give a quadratic equation $27(1 - e^2)^2 s^4 - 2(1 - 9e^2)s^2 - e^2 = 0$ that gives

$$s_1^2 = \frac{1 - 9e^2 + \sqrt{(1 - 9e^2)^2 + 27e^2(1 - e^2)^2}}{27(1 - e^2)^2}, \quad (40)$$

for $0 \leq e < 1$, and $s_1^2 = 1/16$ for $e = 1$. Equation (40) representing $k^2 = 1$ gives the upper boundary (for the values of s) of Region I (the uppermost heavy solid line in Fig.1); it extends from $s_1 = \sqrt{2/27} = 0.272166$ for $e = 0$ to $s_1 = 1/4 = 0.250000$ for $e = 1$, i.e. a line that is nearly parallel to the e -axis. Thus Region I is a region bounded by $0 \leq e \leq 1$, and by $0 \leq s \leq s_1$ where s_1 is given by eq.(40), in which the squared modulus of the elliptic functions that describe the orbits cover the entire range $0 \leq k^2 \leq 1$.

We now use eq.(38) to give a plot of lines of constant $k^2 = 0.001, 0.01, 0.1, 0.3, \dots, 1$ as shown in Fig.1. These lines conveniently divide Region I into regions of increasing field strengths as k^2 increases from 0 to 1. On a point representing a particular k^2 and a particular e value, s can be determined from eq.(38) and the orbit is then given by eq.(20) using eqs.(98), (10) and (21). The values of s on these constant k^2 lines for the values of $e = 0.1, 0.2, \dots, 1.0$ are given in Table 1 which thus give the coordinates (e, s) of the points on the lines representing different values of k^2 . These coordinate points (e, s) from Table 1 are used to

give the following tables: Tables 2 and 3 give the values of q_{\max} and q_{\min} for the orbits obtained from eqs.(26) and (27). Note that the dimensionless distance q is in units of the Schwarzschild radius α which depends on the mass M of the star or blackhole corresponding to that particular coordinate point, and thus one should not compare q at two different coordinate points just by their absolute values alone. Table 4 presents the values of the precession angle in units of π , i.e. $\Delta\phi/\pi$, obtained from eq.(25). Table 5 presents the values of the true eccentricity ε obtained from eq.(28). Tables 2-5 are to be used in conjunction with Table 1 for identifying the locations (e, s) of the corresponding quantities that are presented. The physical quantities presented in Tables 2-5 together with the coordinates (e, s) given in Table 1 now give all possible periodic orbits in the Schwarzschild geometry in its entirety. That is, the coordinates (e, s) of a planet orbiting a non-spinning blackhole can be identified if the observation data on $r_{\min}, r_{\max}, \varepsilon$ and $\Delta\phi$ can be collected. Region I shown in Fig.1 is where orbits given by eqs.(20) and (29) apply. In Sections 4 and 5, we shall discuss Regions II and II' which are shown above Region I in Fig.2 where orbits given by eq.(36) apply. As an example of application of Tables 1-5, from the second row and second column of Tables 1-5 and using only two significant figures, for orbits with $e = 0.10, s = 0.11, k^2 = 0.010$, we find from Tables 2-5 that $q_{\max} = 50, q_{\min} = 34, \Delta\phi/\pi = 0.079$ or $\Delta\phi = 14^\circ$, and $\varepsilon = 0.19$, i.e. orbits with those seemingly small values of s and k^2 give a precession angle of 14° per revolution that is already very large compared to those encountered in our solar system for which the precession angle is only $3.8''$ per century for the earth's orbit (for which $s \simeq 0.983 \times 10^{-4}, k^2 \simeq 0.657 \times 10^{-9}, \varepsilon \simeq e \simeq 0.017$), and the value of the true eccentricity ε of these orbits is already quite different from their energy parameter e . We thus appreciate that the range of values for s given by $0 \leq s \leq s_1$ for Region I, where s_1 ranges from 0.276166 for $e = 0$ to 0.25 for $e = 1$, is not as small as it seems (noting also that $0 \leq k^2 \leq 1$), and that the classical Newtonian orbits are restricted to a very narrow strip of the region indeed for which $s \simeq 0$ and $k^2 \simeq 0$, and for which $\varepsilon \simeq e$ for $0 \leq e \leq 1$.

Although the lines of constant k^2 in Region I conveniently associate the orbits with the orbit equations for the periodic and terminating orbits given by eqs.(20) and (29) and with the physical parameters given in Tables 2-5, the precession angle $\Delta\phi$ and the true eccentricity ε are more physically meaningful parameters that can be associated with the description of the orbit. The expressions for $\Delta\phi$ and ε in terms of k and s are given by eq.(99) in Appendix A and eq.(100) in Appendix B. For a given value of $\Delta\phi$ and of e , we can use eqs.(99) and (38) to solve for s (and k) (using a numerical program such as FSOLVE in MAPLE) and thus locate its coordinate (e, s) ; and similarly for a given value of ε and of e , we can use eqs.(100) and (38) to solve for s (and k). The relationship of e and s with ε is simpler for $k^2 = 1$ and will be discussed later (see eqs.(49) and (50)). In Fig.3, we present lines of constant $\Delta\phi/\pi$ (that are nearly horizontal) and lines of constant ε (that are bent vertical) in Region I, and the corresponding tables for their coordinates are presented in Tables 6 and 7. We note that because $\Delta\phi$ given by eq.(25) depends on γ given by eq.(21) as well as on $K(k)$, the line of constant $\Delta\phi$ does not coincide with the line of constant k^2 except for

$k^2 = 1$. We note also that the line of constant ε does not coincide with the (vertical) line of constant e except for $\varepsilon = e = 1$. We show in Appendix B that it is only for a very thin strip of region, where s is between zero and some very small positive value, that $\varepsilon \simeq e$ which applies in the Newtonian limit. We also show in Appendix B that $\varepsilon = e$ when $e = 1$ exactly. The distinction between e defined by eq.(11) or eq.(13) with ε defined by eq.(28) in the Newtonian or non-Newtonian theory has never been clearly recognized previously.

With Fig.3 which has curves of constant $\Delta\phi/\pi$ and constant ε in place, Region I is now partitioned into cells with the coordinate points specified by $(\Delta\phi/\pi, \varepsilon)$. We have a clear idea what the orbits of a planet would be like at points within each cell in terms of their precession angle and true eccentricity, and the coordinates of these orbits (e, s) then give the energy and field parameters corresponding to these orbits. In Fig.4, we present examples of periodic and unbounded orbits, plotted in polar coordinates (q, ϕ) , corresponding to various precession angles of $\pi/6, \pi/3, \pi/2, \pi, 3\pi/2, 2\pi, \infty$ (vertically from top to bottom) for values of $e = 0, 0.5, 1$ (horizontally from left to right), where the star or blackhole is located at the origin. We first note that the orbits for which $e < 1$ are periodic and closed because f is a rational number in $\Delta\phi = f\pi$ for each one of them. The precession angle can be seen from the heavy solid line that marks the trajectory (as ϕ increases) from the initial point at $\phi = 0$ to the first point at which the distance from the origin is equal to the distance at $\phi = 0$. The true eccentricity of the orbits is ε given by eq.(28). For example, for the orbit of Fig.4 (a1) for $\Delta\phi = \pi/6, e = 0, \varepsilon$ is far from zero which can be seen from the q_{\min} and q_{\max} in the figure, and it can be more accurately calculated to be equal to 0.22629. For each of the unbounded orbits characterized by $e = 1$, the incoming trajectory coming from infinity at $\phi = 0$ makes an angle ϕ with the outgoing trajectory going to infinity given by $\phi = 2K(k)/\gamma = 2\pi + \Delta\phi$ from eq.(25), as can be seen in some of the figures presented. The case $\Delta\phi/\pi = \infty$ corresponding to the special case of $k^2 = 1$ will be discussed later in this section for which the planet starting from q_{\max} ends up circling the blackhole with a radius that approaches q_{\min} (see Fig.6d).

Generally, if we are given a coordinate point in Fig.3, for example, a point on $e = 0.5$ just above the $\Delta\phi/\pi = 1/3$ line slightly to the left of the $\varepsilon = 0.6$ curve (where $\varepsilon = 0.581431\dots$ and $s = 0.194229\dots$), then we find $\Delta\phi = 60.4706\dots$ degrees or $\Delta\phi/\pi = 0.33594\dots$, and part of the orbit is shown in Fig.5. Whether the orbit will close on itself depends on whether $\Delta\phi/\pi$ is or is not a rational number in principle, even though, as we mentioned before, a truncated number in practice is always a rational number and the orbit will be a closed one. We only show part of the orbit in Fig.5 as the subsequent path is clear from the angle of precession and true eccentricity of the orbit and we are not concerned with how many "leaves" the orbit is going to create. Figure 3 (or one with even more curves of constant $\Delta\phi/\pi$ and constant ε) is a very useful map that can be used fruitfully with any observation data that are obtained for any planet.

Besides the special case $k^2 = 1$, the case of $k^2 = 1/2$ is also somewhat special in that it allows many relationships to be expressed simply and explicitly. We present some of these simple relations for $k^2 = 1/2$ in Appendix C. It is to be

noted from Fig.1 that the line of constant $k^2 = 1/2$ is very close to the boundary given by $k^2 = 1$. The line of constant $k^2 = 1/2$ for Region II, on the other hand, is closer to dividing the region approximately into two halves, as shown in Fig.2. The $k^2 = 1/2$ curve for Region II will be discussed in Section 4.

The terminating orbits in Region I given by eq.(29) can be characterized by the planet's initial position q_1 given by eq.(31), and by the angle ϕ_1 at which the planet enters the center of the blackhole. It is interesting to note that even for these terminating orbits, the precession angle still has an "extended" meaning and use that we shall describe. It is clear from eq.(29) that the orbit terminates, i.e. q becomes zero when $\gamma\phi_1 = K(k)$, but if the orbit is continued (by continuing to increase ϕ), q would assume its initial value at $\phi = 0$ when $\gamma\phi' = 2K(k)$, producing a "precession angle" of $\Delta\phi = \phi' - 2\pi = 2K(k)/\gamma - 2\pi$ which is equal to the precession angle for the corresponding periodic orbit at the same coordinate point (e, s) . Since $\phi' = 2\phi_1$, the polar angle ϕ_1 at which the path of the terminating orbit enters the center of the blackhole is related simply to the precession angle of the periodic orbit by $\phi_1 = \Delta\phi/2 + \pi$, or

$$\frac{\phi_1}{\pi} = \frac{1}{2} \frac{\Delta\phi}{\pi} + 1.$$

As ϕ_1/π can be easily calculated from $\Delta\phi/\pi$ for the periodic orbits given in Table 4, we do not tabulate it separately. The values of q_1 are presented in Table 8, and we note the small range $1 \leq q_1 \leq 2.25$ for the entire Region I. Examples of these terminating orbits are presented in Fig.6. The dotted line represents the continuation of the orbit when ϕ is continued beyond ϕ_1 .

Before we discuss Regions II and II', we want to describe three special cases: the case of $k^2 = 0$ which, as we shall see, is not of any interest but must be included for completeness; the case of $k^2 = 1$ which gives the upper boundary of Region I (and lower boundary of Region II); and the case of $e = 1$ which gives the right boundary of Region I (and of Regions II and II') (see Figs.1 and 2).

(i) The Special Case of $k^2 = 0$

The line of $k^2 = 0$ coincides with the $s = 0$ axis in Fig.1. To show this, we note that $k^2 = 0$ implies $\theta = 0$ from eq.(95). Substituting $\theta = 0$ into eq.(24) gives $s = 0$ when we use the expressions in eq.(10) for g_2 and g_3 . The we find $g_2 = 1/12$ and $g_3 = 1/216$, and from eq.(98), we find

$$\begin{aligned} e_1 &= \frac{1}{6}, \\ e_2 &= e_3 = -\frac{1}{12}. \end{aligned}$$

Equation (20) then gives $1/q = 0$ or $q = \infty$, i.e. it is the limiting case of zero gravitational field. As we pointed out earlier, the classical Newtonian case is given by only a very narrow strip represented by $k^2 \simeq 0$ and $s \simeq 0$ for which q is large but finite.

(ii) The Special Case of $k^2 = 1$

It follows from eqs.(38) and (39) that on the line of $k^2 = 1$, $\cos \theta = -1$. Thus from eqs.(24) and (17), we have

$$\Delta = 0 \quad (41)$$

which can be identified as the "boundary" between Solutions A and B in Section 2. The range of s values for $\Delta = 0$ is $0.25 \leq s \leq 0.272166$ for $1 \geq e \geq 0$ (see the discussion below eq.(40)), and for that range of s values, $s \leq 1/2\sqrt{3} = 0.288675$ or $s^2 \leq 1/12$ and therefore $g_2 > 0$ (see eq.(10)). From eq.(41), the relation between g_2 and g_3 can be more precisely expressed as

$$\sqrt[3]{g_3} = -\sqrt{\frac{g_2}{3}}$$

after noting that g_3 is negative and g_2 is positive for the values of s along the line $k^2 = 1$. Also from eq.(98), we note that

$$\begin{aligned} e_1 &= e_2 = \sqrt{\frac{g_2}{12}}, \\ e_3 &= -\sqrt{\frac{g_2}{3}}. \end{aligned} \quad (42)$$

The periodic orbits given by eq.(20) become

$$\frac{1}{q} = \frac{1}{3} + 2\sqrt{\frac{g_2}{3}} \frac{1 - 5 \sec h(2\gamma\phi)}{1 + \sec h(2\gamma\phi)}, \quad (43)$$

where

$$\gamma = \left(\frac{3g_2}{4}\right)^{1/4} \quad (44)$$

and where the values of g_2 (and g_3) are those given by the values of e and s on the line $k^2 = 1$ that are obtained from eq.(40). The orbit is not a periodic orbit; it is what we call an asymptotic periodic orbit. The planet starts from an initial position q_{\max} at $\phi = 0$ given by

$$\frac{1}{q_{\max}} = \frac{1}{3} + 4e_3 = \frac{1}{3} - 4\sqrt{\frac{g_2}{3}} \quad (45)$$

and ends up at $\phi = \infty$ circling the star or blackhole with a radius that asymptotically approaches q_{\min} given by

$$\frac{1}{q_{\min}} = \frac{1}{3} + 4e_2 = \frac{1}{3} + 2\sqrt{\frac{g_2}{3}}. \quad (46)$$

Equations (43)-(46) are explicit and simple equations that give the orbit equation, q_{\max} , and q_{\min} for $k^2 = 1$. In particular, it is seen from Table 3, for example, that q_{\min} ranges from 2 for $e = 0$ to $9/4 = 2.25$ for $e = 1$, i.e. q_{\min} is

still no less than twice the Schwarzschild radius for the strongest gravitational field that permits the periodic orbits. However, it is a very small number indeed compared to, say, $q_{\min} \simeq 5 \times 10^7$ for the earth's orbit around the sun.

On this upper boundary $k^2 = 1$ of Region I, the terminating orbit given by eq.(29) from Solution A2 becomes a circular orbit with a radius $q_c = q_1$, where q_1 is the initial distance of the planet from the star or blackhole given by eq.(30). From eqs.(30) and (31) and noting that $e_1 = e_2$ for $k^2 = 1$, we find that

$$q_c = q_1 = q_{\min} \quad (47)$$

given by eq.(46) (see Tables 3 and 8 for $k^2 = 1$). We shall refer to the orbits given by eqs.(43) and (47) as the asymptotic periodic and the asymptotic terminating orbits respectively of Region I. Thus the special cases given by eqs.(43) and (47) for $k^2 = 1$ of the periodic and terminating orbits given by eqs.(20) and (29) for solutions A1 and A2 respectively clearly exhibit completely different behaviors from their counterparts for $0 \leq k^2 < 1$. Examples of asymptotic periodic orbits are shown in Fig.4g. Asymptotic terminating orbits are simply circles of radius equal to q_1 , as shown in Fig.6(d).

Using eqs.(28), (42), (45) and (46), for $k^2 = 1$ the true eccentricity ε can be shown to be expressible in terms of g_2 by

$$\varepsilon = \frac{9\sqrt{g_2/3}}{1 - 3\sqrt{g_2/3}}, \quad (48)$$

which can be solved to give s in terms of ε , and then e in terms of ε using eq.(38). We find that the coordinates (e, s) of a given $0.6 \leq \varepsilon \leq 1$ on the line $k^2 = 1$ are given by

$$e = \frac{\sqrt{(1+\varepsilon)(-3+5\varepsilon)}}{(3-\varepsilon)}, \quad (49)$$

and

$$s = \frac{\sqrt{(3-\varepsilon)(1+\varepsilon)}}{2(3+\varepsilon)}. \quad (50)$$

It is interesting that eqs.(49) and (50) can be used in place of eq.(40) as parametric equations for determining the coordinates (e, s) of the line $k^2 = 1$ as ε takes the values from 0.6 to 1. In particular, eqs.(49) and (50) allow us to see that the $\varepsilon = \text{const.}$ curves are not vertical (except for $\varepsilon = e = 1$), and they intersect the upper boundary s_1 of Region I for $0.6 \leq \varepsilon \leq 1$ (see Fig.3). The $\varepsilon = 0.6$ curve, the boundary curve s_1 , and the s -axis are concurrent at $e = 0, s = \sqrt{2/27}$. We can conclude that periodic orbits with $e = 0$ have true eccentricity in the range $0 \leq \varepsilon \leq 0.6$. As another example it can be shown using eqs.(49) and (50) that periodic orbits with $e < 3\sqrt{5}/11 = 0.609836$ have $\varepsilon < 0.8$.

(iii) The Special Case of $e = 1$

The maximum or boundary value for e which is $e = 1$ is also a special case of interest. From its definition given by eq.(11), since $\kappa^2 \leq 1$, e cannot be greater than 1. In Appendix B, we show that $e = 1$ always gives an unbounded orbit for the periodic and the asymptotic periodic orbits of Region I and the terminating orbits of Region II, but not the asymptotic terminating orbit of Region I which has a radius given by eq.(47) independent of e and thus is not an unbounded orbit. Thus $e = 1$ is the boundary for e for Region I (as well as for Region II). Many explicitly simple relationships among s, k, q_{\min}, q_1 , etc. have been found on the boundary line $e = 1$, and they are given and proved in Appendix B. In particular, we have, on $e = 1$ in Region I, that

$$s^2 = \frac{k^2}{4(1+k^2)^2}, \quad (51)$$

$$\gamma = \left(\frac{1}{4(1+k^2)} \right)^{1/2}, \quad (52)$$

$$q_{\min} = \frac{1+k^2}{k^2}, \quad (53)$$

and

$$q_1 = 1 + k^2. \quad (54)$$

Examples of unbounded orbits for $e = 1$ are shown in Fig.4 (a3-g3).

We shall now describe Regions II and II' for the orbit equation (36) given by solution B for the case $\Delta > 0$.

4 Region II

Consider the orbits expressed by eq.(36) given by solution B and characterized mathematically by $\Delta > 0$. The associated values for (e, s) in this case satisfy $s > s_1$, where s_1 is the upper boundary of Region I given by eq.(40). This region of parameter space defined by $s > s_1$ can be naturally divided into two sectors which we call Region II and II' with Region II bordering Region I (see Fig.2). The boundary between Regions II and II' is determined by the Schwarzschild radius in a manner to be described later in this section.

We first want to prove that the lower boundary (for s) of Region II, characterized by $\Delta = 0$ as it is for the upper boundary of Region I, also gives $k^2 = 1$, where k^2 is calculated from eq.(35) for Solution B (In Section 3, we showed that for k^2 calculated from eq.(22) for Solution A, $k^2 = 1$ implies $\Delta = 0$). Substituting $\Delta = 0$ into eq.(32) gives

$$A = B = \frac{1}{2} \sqrt[3]{g_3} = -\frac{1}{2} \sqrt{\frac{g_2}{3}}.$$

After noting that $A(= B)$ is a negative value for the range of s values for $\Delta = 0$, substituting the above into eq.(35) gives $k^2 = 1$. We also find from

eq.(34) that $\gamma^2 = -3\sqrt[3]{g_3}/2 = \sqrt{3g_2}/2$ which agrees with the γ given by eq.(44), and we find from eq.(33) that

$$a = \sqrt[3]{g_3} = -\sqrt{\frac{g_2}{3}}. \quad (55)$$

Substituting these into eq.(36) gives the same orbit equation (43) for the terminating orbit in Region II on its lower boundary as that for the asymptotic periodic orbit in Region I on its upper boundary. Thus on the boundary $k^2 = 1$ the equation for the orbits in Region II does not represent a terminating orbit but is the same as the asymptotic periodic orbit for Region I given by eq.(43) (see Fig.4, g1-g3). Also, from eqs.(42) and (55), we see that the smallest root in eq.(23) in Solution (A) is identified with the real root given by eq.(33) of Solution (B), i.e. $e_3 = a$. Thus from eqs.(26) and (37), $q_2 = q_{\max}$ when $k^2 = 1$, i.e. the initial distance q_2 of the terminating orbit in Region II can be identified as the continuation of q_{\max} of the periodic orbit from Region I. On the boundary of Regions I and II, the two other real roots $e_1 = e_2$ given by eq.(42) of the cubic equation (16) agree with $b = \bar{b}$ given below eq.(33). The line $k^2 = 1$ defined by eq.(40) is the boundary between Regions I and II; it is the upper boundary for Region I and is the lower boundary for Region II (see Fig.2). The above discussion also illustrates the transition that takes place: from a periodic orbit to an asymptotic periodic orbit to a terminating orbit, as one crosses the boundary from Region I to II.

We now consider the upper boundary of Region II. We define this boundary to be that obtained by requiring the planet's initial position to be just at the Schwarzschild horizon, i.e. that obtained by setting $q = 1$ initially at $\phi = 0$. Setting $q = 1$ in eq.(36) for $\phi = 0$ which is $1/q = 1/3 + 4a$, we require $a = 1/6$, where a is the real root of the cubic equation (16). We then use the equation

$$4\left(\frac{1}{6}\right)^3 - \left(\frac{1}{6}\right)g_2 - g_3 = 0, \quad (56)$$

and substitute the expressions for g_2 and g_3 given in eq.(10) into eq.(56) and solve for s . We find

$$s_2^2 = \frac{1}{1 - e^2} \quad (57)$$

which we shall use as the equation for the upper boundary of Region II, for $0 \leq e \leq 1$. Thus Region II is a region bounded between $e = 0$ and $e = 1$, and between s_1 given by eq.(40) (the lower heavy solid line in Fig.2) and s_2 given by eq.(57) (the upper heavy solid line in Fig.2), i.e. $s_1 < s \leq s_2$. The region defined by $s_2 < s \leq \infty$ and bounded between $e = 0$ and $e = 1$ will be called Region II', for which the planet's initial position ranges from just inside the Schwarzschild horizon up to the center of the blackhole. Since the same terminating orbit equation (36) applies in Regions II and II', the division into two regions may seem unnecessary. However, the Schwarzschild radius is of physical significance, and it is useful to know the location of the curve s_2 in the (e, s) plot which

indicates that the initial position of the planet is at the Schwarzschild horizon. Separating out Region II' also makes it possible to realize and appreciate that a very large region of the characterizing parameter $s_2 < s \leq \infty$ is of relevance only to a very small physical region $0 \leq q < 1$ for the case where the initial position of the planet is inside the Schwarzschild horizon.

For Region II, as s increases its value above those on its lower boundary $s = s_1$ on which $k^2 = 1$, the value of k^2 calculated from eq.(35) decreases from 1. The curves of constant k^2 for $k^2 = 0.9, 0.8, \dots$ can be easily obtained from eq.(35) where A and B are expressed in terms of s and e (again using MAPLE FSOLVE) and they are presented in Fig.2. However, the value of k^2 has a minimum value that is not 0 in Region II. First, we show in Appendix C that the $k^2 = 1/2$ curve is given by

$$s^2 = \frac{1}{6(1-e^2)} \left(1 + \sqrt{\frac{1+2e^2}{3}} \right). \quad (58)$$

The significance of this $k^2 = 1/2$ curve is that on it, as $e \rightarrow 1$, $s \rightarrow \infty$, just like the curve for the upper boundary of Region II represented by eq.(57). For $k^2 > 0.5$, the constant k^2 curves intersect the $e = 1$ line at some finite value of s , whereas for $k^2 < 0.5$, the constant k^2 curves intersect the upper boundary curve given by eq.(57) at points for which the values of e are less than 1. We then find that the minimum value of k^2 in Region II is equal to $1/2 - 1/(2\sqrt{5}) = 0.276393$ which is obtained by setting $e = 0$, $s = 1$ in eqs.(32) and (35), and this value of k^2 appears at one coordinate point only at $e = 0$ and $s = 1$. There is no orbit whose k^2 is less than 0.276393 in Region II (see Fig.2), and k^2 is thus restricted to the range $0.276393 \leq k^2 \leq 1$.

In Table 9, we present the coordinates (e, s) of these curves of constant k^2 between 0.276393 and 1. In Table 10, we present the values of q_2 given by eq.(37), the initial distance of the planet from the blackhole. Note that unlike q_1 for the terminating orbits in Region I whose range is finite and small, q_2 can be infinite (for $e = 1$ and $k^2 > 0.5$). Like the terminating orbits of Region I, the terminating orbits of Region II can be characterized by q_2 and the angle ϕ_2 at which the planet enters the center of the blackhole. If we define the "precession angle" $\Delta\phi$ for the terminating orbits as in eq.(25), with k and γ defined by eqs.(35) and (34), then $\phi_2 = K(k)/\gamma = \Delta\phi/2 + \pi$, or

$$\frac{\phi_2}{\pi} = \frac{1}{2} \frac{\Delta\phi}{\pi} + 1. \quad (59)$$

In Table 11, we present the values of ϕ_2 . Tables 10 and 11 are to be used in conjunction with Table 9 that give the coordinates of the constant k^2 curves. Examples of these terminating orbits obtained from eq.(36) are shown in Fig.7(b)-(d). Again the dotted line shows the continuation of the orbit beyond ϕ_2 . A planet coming from very far away, i.e. an unbounded orbit with $e = 1$, with an initial trajectory perpendicular to the line joining it to the blackhole, can terminate at the blackhole; the condition for this to happen is $s > 0.25$. Figures 8 (a)-(c) show three unbounded orbits ($e = 1$) as s increases from just below

to just above the critical field parameter $s = 0.25$. Figure 8(a) also shows an example of a precession angle in which the planet makes more than three revolutions around a blackhole before assuming a distance equal to its initial distance (which is infinity) from the blackhole. As noted after eq.(25), the actual precession angle in this case should be more appropriately given by $2K(k)/\gamma - 6\pi$ which can be obtained from the presented value of $\Delta\phi/\pi = 4.6378$ (where $\Delta\phi$ is defined by eq.(25)) and gives 0.6378π . Thus for Fig.8(a), 0.6378π gives the angle between the initial incoming trajectory from very far away at $\phi = 0$ and the final outgoing trajectory going to infinity, i.e. 0.6378π is the polar angle of the direction of the outgoing trajectory going to infinity with respect to the x -axis (but we have not extended the outgoing trajectory far enough to show the accuracy of this angle).

We now present some useful simple expressions for the following special cases.

(i) Special Case on the Upper Boundary of Region II Given By Eq.(57)

We show in Appendix D that on the upper boundary of Region II given by eq.(57), the values of k^2 and γ given by eqs.(35) and (34) become

$$k^2 = \frac{1}{2} - \frac{1}{4\sqrt{1/3 - g_2}}, \quad (60)$$

$$\gamma = \left[\frac{1}{4} \left(\frac{1}{3} - g_2 \right) \right]^{1/4}, \quad (61)$$

where the s values for g_2 are given by eq.(57).

(ii) Special Case on the Right Boundary $e = 1$ of Region II

Just as for Region I, there are simple and interesting relations among k^2 , s and γ on the right boundary $e = 1$ of Region II, and they are shown in Appendix D. In particular, we have, on $e = 1$ in Region II, that for $s > 1/4$,

$$k^2 = \frac{1}{2} + \frac{1}{8s}, \quad (62)$$

or that, for $1 \geq k^2 > 1/2$,

$$s = \frac{1}{8(k^2 - 1/2)}, \quad (63)$$

and that

$$\gamma = \sqrt{\frac{s}{2}}. \quad (64)$$

Appendix D also presents a special case given by $s^2 = 1/12$ that is notable.

5 Region II'

While we may call the entire sector $s > s_1$ given by eq.(40) above Region I in Fig.2 just one region that allows only terminating orbits given by eq.(36),

it is useful to divide it into Regions II and II' using the curve $s = s_2$ given by eq.(57). Region II' is the region of parameter space in (e, s) for which $s > s_2$ and $0 \leq e < 1$. The heavy solid curve labeled s_2 in Fig.2 delineates the boundary of Region II' which separates it from Region II. Despite the apparent large size of Region II', the terminating orbits here have little variety in the sense that the range of initial distances $q_{2'}$ that are given by $1/q_{2'} = 1/3 + 4a$ (see eq.(37)), is limited ($0 \leq q_{2'} < 1$) and the range of the angle $\phi_{2'} = K(k)/\gamma$ at which the planet enters the blackhole is also limited. It can be shown that the range of $\phi_{2'}$ is $0 \leq \phi_{2'} < 0.789\pi$. An example of a terminating orbit obtained from eq.(36) in Region II' is shown as the solid line in Fig.7(e); the dotted line shows the continuation of the orbit beyond $\phi_{2'}$. It may be of some mathematical interest to note that as $s \rightarrow \infty$ in Region II', the modulus of the Jacobian elliptic functions used to describe the orbits does not go to zero; instead $k^2 \rightarrow (2 - \sqrt{3})/4 = 0.0669873$, and thus k^2 in Region II' is restricted to the range $0.0669873 \leq k^2 < 0.5$.

Tables 1-8, the orbit equations (20), (29) and (36), and the description of the orbits and the three regions where these orbit equations apply, complete our characterization of all possible planetary orbits in the Schwarzschild geometry.

We now briefly discuss how all this may be used for the Kerr geometry when the spinning blackhole has a spin angular momentum per unit mass of the blackhole that is relatively small compared to the orbital angular momentum per unit mass of the planet.

6 Kerr Geometry

The spinning blackhole is assumed to have a spin angular momentum J given by [1]

$$J = Mac, \quad (65)$$

where ac can be identified as the spin angular momentum per unit mass of the blackhole and is the quantity to be compared with h , the orbital angular momentum per unit mass of the planet. The Kerr geometry becomes the Schwarzschild geometry in the limit $ac/h \rightarrow 0$.

The worldline of a particle moving in the equatorial plane $\theta = \pi/2$ satisfies the equations [1]

$$\dot{t} = \frac{1}{D} \left[\left(r^2 + a^2 + \frac{\alpha a^2}{r} \right) \kappa - \frac{\alpha a h}{cr} \right], \quad (66)$$

$$\dot{\phi} = \frac{1}{D} \left[\frac{\alpha a c \kappa}{r} + \left(1 - \frac{\alpha}{r} \right) h \right], \quad (67)$$

where $D \equiv r^2 - \alpha r + a^2$. For the equatorial trajectories of the planet in the Kerr geometry, the combined energy equation is

$$\frac{1}{r} + \frac{h^2 - a^2 c^2 (\kappa^2 - 1)}{r^2} - \frac{\alpha (h - a c \kappa)^2}{r^3} - \frac{c^2 \alpha}{r} = c^2 (\kappa^2 - 1). \quad (68)$$

Provided that $a^2/\alpha^2 < 1$ and $ack/h \ll 1$, to the first order in ack/h , it is not difficult to see, by comparing eqs.(66)-(68) with eqs.(3)-(6), that we can re-scale α to $\alpha' = \alpha(1 - 2ack/h)$, s to $s' = s(1 - ack/h)$, and ϕ to $\phi' = \phi[1 - b(ack/h)]$, where b is some approximation constant, such that the results we have presented for the orbits in the Schwarzschild geometry are approximately applicable for the orbits in the Kerr geometry in terms of the scaled parameters. That is, the orbits in the equatorial plane and their characterization for the Schwarzschild and Kerr geometries are qualitatively very similar to the first order in ack/h except that the basic parameters s , α and ϕ have to be slightly rescaled. Levin and Perez-Giz [5] obtained their orbits in the Kerr geometry from numerically integrating eqs.(66)-(68) and it would be interesting to study and examine when and how the planet's orbits in the Kerr geometry that they obtained can be related with our results with the scaled parameters, and when and how they begin to differ significantly from those in the Schwarzschild geometry that we presented in this paper.

7 Trajectory of Light

We now consider the deflection of light by a gravitational field. We cannot use the proper time τ as a parameter. So we use some affine parameter σ along the geodesic [1]. Considering motion in the equatorial plane, the geodesic equations give eqs.(3) and (5), and we replace the r -equation (4) by the first integral of the null geodesic equation, and we have [1]

$$\left(1 - \frac{\alpha}{r}\right) \dot{t} = \kappa, \quad (69)$$

$$c^2 \left(1 - \frac{\alpha}{r}\right) \dot{t}^2 - \left(1 - \frac{\alpha}{r}\right)^{-1} \dot{r}^2 - r^2 \dot{\phi}^2 = 0, \quad (70)$$

$$r^2 \dot{\phi} = h, \quad (71)$$

where the derivative $\dot{}$ represents $d/d\sigma$. Substituting eqs.(69) and (71) into (70) gives the 'combined' energy equation

$$\dot{r}^2 + \frac{h^2}{r^2} \left(1 - \frac{\alpha}{r}\right) = c^2 \kappa^2. \quad (72)$$

Substituting $dr/d\sigma = (dr/d\phi)(d\phi/d\sigma) = (h/r^2)(dr/d\phi)$ and $u = 1/r$ into the combined energy equation gives the differential equation for the trajectories of light in the presence of a gravitational field

$$\left(\frac{du}{d\phi}\right)^2 = \alpha u^3 - u^2 + \frac{c^2 \kappa^2}{h^2}. \quad (73)$$

The constants κ and h have a physical significance through their ratio κ/h as follows: Let R denote the distance of the light beam to the center of a star or

blackhole when the trajectory of the light beam is such that $du/d\phi = 0$. R can either be associated with the distance of closest approach of the light beam to the blackhole or with the initial distance to the blackhole of the light beam. The latter case is associated with light trajectories that terminate at the blackhole. With R so defined and letting $u_1 \equiv 1/R$, we can set $c^2\kappa^2/h^2$ to be equal to $u_1^2 - \alpha u_1^3$ [8].

It is again convenient to consider the problem in terms of the dimensionless inverse distance U defined by

$$U = \frac{\alpha}{r} = \alpha u = \frac{1}{q}. \quad (74)$$

U defined here is slightly different from the U defined by eqs.(8) and (19) previously. In terms of U of eq.(74), eq.(73) becomes

$$\left(\frac{dU}{d\phi}\right)^2 = U^3 - U^2 + \frac{c^2\kappa^2\alpha^2}{h^2}. \quad (75)$$

Since $dU/d\phi = 0$ at $r = R$, one root U which we call

$$U_1 \equiv \frac{\alpha}{R} \equiv \alpha u_1 \quad (76)$$

of the cubic equation $U^3 - U^2 + c^2\kappa^2\alpha^2/h^2 = 0$ is known, and the term $c^2\kappa^2\alpha^2/h^2$ on the right hand side of eq.(75) can be replaced by $-U_1^3 + U_1^2$, and the other two roots of the cubic equation $U^3 - U^2 - U_1^3 + U_1^2 = 0$ can be found from solving a quadratic equation. We denote the three roots of the cubic equation by e_1, e_2, e_3 . Thus writing eq.(75) as

$$\left(\frac{dU}{d\phi}\right)^2 = U^3 - U^2 - U_1^3 + U_1^2 \quad (77)$$

the trajectory of light represented by an equation for U as a function of the polar angle ϕ obtained from integrating eq.(77) can be characterized by a single parameter U_1 which essentially specifies either the distance of the closest approach or the initial distance of the light beam to the blackhole (These distances are scaled by the Schwarzschild radius of the blackhole). As in our discussion of the planets, our references to the initial position of the light beam assume that the trajectory of the light beam at that initial position is perpendicular to the line joining that position to the star or blackhole. The range of U_1 is clearly between 0 and ∞ , where $U_1 = 0$ means that the light beam is infinitely far away from the blackhole, $U_1 = 1$ means that the light beam is at the Schwarzschild radius at its closest approach or its initial position, and $U_1 = \infty$ means that the light beam is at the center of the blackhole. As we show in the following, the region $0 \leq U_1 \leq \infty$ can be appropriately divided into three sectors which we again call Regions I, II and II'. The similarity between the characterization of these three regions with that for the planetary orbits discussed in the previous sections will become apparent. Not surprisingly perhaps, only a single parameter which we choose to be U_1 , is needed for the characterization of the

trajectories of a light beam in contrast to the two parameters (which we choose to be e and s), which we needed for the characterization of the orbits of a planet. The relationship between U_1 and R , from eqs.(76) and (2), is

$$R = \frac{2}{U_1} \left(\frac{GM}{c^2} \right).$$

Region I: $0 \leq U_1 \leq 2/3$, or $\infty > R \geq 3GM/c^2$

Here R denotes the distance of closest approach of a light beam that comes from a great distance. We let

$$\begin{aligned} e_1 &= \frac{1}{2}[1 - U_1 + (1 + 2U_1 - 3U_1^2)^{1/2}], \\ e_2 &= U_1, \\ e_3 &= \frac{1}{2}[1 - U_1 - (1 + 2U_1 - 3U_1^2)^{1/2}], \end{aligned} \quad (78)$$

with $e_1 > e_2 > e_3$, and we consider the region $e_1 > e_2 > U \geq e_3$, and write eq.(77) as

$$\left(\frac{dU}{d\phi} \right)^2 = (e_1 - U)(e_2 - U)(U - e_3). \quad (79)$$

Equation (79) can be integrated [7] with ϕ expressed in terms of an inverse sn function. After a little algebra and re-arrangement, we find the trajectory's equation in terms of the Jacobian elliptic functions of modulus k to be

$$\frac{1}{q} = \frac{(e_1 - e_3)e_2 - (e_2 - e_3)e_1 sn^2(\gamma\phi, k)}{(e_1 - e_3) - (e_2 - e_3)sn^2(\gamma\phi, k)}, \quad (80)$$

where

$$\begin{aligned} \gamma &= \frac{(e_1 - e_3)^{1/2}}{2}, \\ k^2 &= \frac{e_2 - e_3}{e_1 - e_3}. \end{aligned} \quad (81)$$

The angle of deflection $\Delta\phi$ can be obtained as follows. If we set $q = \infty$ and also set $\phi = \pi/2 + \Delta\phi/2$ as the incoming angle in eq.(80) (see Fig.9a for the special case of $\Delta\phi/2 = 45^\circ$) where $\Delta\phi$ denotes the total angle of deflection of light by the mass M , we get the following equation for determining $\Delta\phi$ exactly:

$$sn^2 \left[\gamma \left(\frac{\pi}{2} + \frac{\Delta\phi}{2} \right), k \right] = \frac{(e_1 - e_3)e_2}{(e_2 - e_3)e_1},$$

where e_1, e_2, e_3, γ, k , are given by eqs.(78) and (81). It can also be expressed as

$$\Delta\phi = -\pi + \frac{2}{\gamma} \text{sn}^{-1}(\psi, k), \quad (82)$$

where

$$\psi = \left[\frac{(e_1 - e_3)e_2}{(e_2 - e_3)e_1} \right]^{1/2}$$

Equations (80)-(82) were first given by one of us in ref.6. Examples of these trajectories obtained from eq.(80) are presented in polar coordinates (q, ϕ) in Fig.9, where the blackhole is located at the origin. By setting the angles of deflection $\Delta\phi$ presented in Fig.9 to be $\pi/2, \pi, 3\pi/2, 2\pi$, the corresponding values of U_1 can be determined from eqs.(82) and (78) using the MAPLE FSOLVE program, and they are found to correspond to the distances of closest approach $R = 4.6596GM/c^2, 3.5206GM/c^2, 3.2085GM/c^2, 3.0902GM/c^2$ respectively. The case of $R = 3.5206GM/c^2$ is interesting as it corresponds to the light ray being turned around by 180° . That the upper boundary of Region I characterized by $U_1 = 2/3$ or $R = 3GM/c^2$ is a very special case can be seen mathematically because it results in $e_1 = e_2 = 2/3, e_3 = -1/3$, and hence $k^2 = 1, \gamma = 1/2$ and $U = 2/3 = \text{const.}$ from eqs.(81) and (80). Physically, it results in the light circling the blackhole with a radius $R = 3GM/c^2$ even though the trajectory has been shown to be an unstable one [1]. This known result can also be simply obtained from the equation of motion $d^2U/d\phi^2 = (3/2)U^2 - U$ for $U = \text{const.}$ and thus $U = 2/3$. If one compares the size of the unstable circular photon orbit with the allowed limiting radii of the planetary asymptotic periodic orbits ($2 \leq q_{\min} \leq 2.25$ or $4GM/c^2 \leq r_{\min} \leq 4.5GM/c^2$), one can see that the radius of the asymptotic circular path of a planet around a blackhole is still a little larger than that for a photon, but not by much.

The lower boundary of Region I characterized by $U_1 = 0$ or $R = \infty$ gives $e_1 = 1, e_2 = e_3 = 0, k^2 = 0$ and $\gamma = 1/2$, and thus gives $U = 0$ or $r = \infty$ which is a limiting case as the light ray that is infinitely far away at its closest approach to the blackhole is completely undeflected.

As in the case of the Region I particle orbits discussed in Section 3, the squared modulus k^2 of the elliptic functions that describe the trajectories of light here also covers the entire range $0 \leq k^2 \leq 1$; it varies from 0 at the lower boundary to 1 at the upper boundary.

For small U_1 , the trajectory of light given by eq.(80) has been shown [6] to reduce to

$$\frac{1}{r} \simeq \frac{\cos \phi}{R} + \frac{GM}{c^2 R^2} (1 + \cos \phi + \sin^2 \phi), \quad (83)$$

and the total deflection of light to reduce to the well known result

$$\Delta\phi \simeq \frac{4GM}{c^2 R}. \quad (84)$$

It can be shown from our exact result given by eq.(82) that this approximate expression (84) still gives an accuracy of two significant figures for $U_1 = 0.1$ or $R = 20GM/c^2$.

As U_1 approaches $2/3$, or as R approaches $3GM/c^2$, we may let $U_1 = 2/3 - \delta$, where $\delta \equiv (2/3)(1 - 3GM/c^2 R)$ is a small positive number. From eqs.(78) and (81), we can express the quantities $2/\gamma$, ψ and k appearing in eq.(82) in power series in δ and find, to the first order in δ , $2/\gamma \simeq 4(1 - \delta/2 + \dots)$, $\psi \simeq 1 - \delta/2 + \dots$, and $k \simeq 1 - \delta + \dots$. Substituting these into eq.(82) immediately gives an expression for $\Delta\phi$ which is correct to the first order in δ . If an attempt is made to find an expansion of $sn^{-1}(\psi, k)$ near $k = 1$, since $sn^{-1}(\psi, 1) = \tanh^{-1}\psi = \ln[(1 + \psi)/(1 - \psi)]^{1/2}$, the expansion would involve terms in $\ln\delta$ (which is a large number for small δ) and ordering the expansion terms in the right way can be tricky. Different forms of such expansions have been given and studied by various authors [9]. As we showed above and in Fig.9, our exact expressions given by eqs.(80) and (82) can be used simply and directly for all cases in Region I.

As U_1 increases beyond $2/3$ or as the distance of closest approach R of the light beam to the blackhole becomes smaller than $3GM/c^2$, the light is not just deflected but is absorbed by and terminates at the blackhole. It is useful to divide the region $2/3 < U_1 \leq \infty$ or $3GM/c^2 > R \geq 0$ into two regions that we call Region II and II' that are separated by the Schwarzschild horizon, as we discuss below. Region II is for R from $3GM/c^2$ up to the Schwarzschild horizon, and Region II' is for R from the Schwarzschild horizon up to the center of the blackhole.

Region II: $2/3 < U_1 \leq 1$, or $3GM/c^2 > R \geq 2GM/c^2$

Here R denotes the initial distance to the blackhole of the light beam which has initial trajectory (as ϕ increases from 0) perpendicular to the line joining it to the blackhole.

As U_1 increases beyond $2/3$, U_1 becomes greater than $[1 - U_1 + (1 + 2U_1 - 3U_1^2)^{1/2}]/2$, and the order of the three roots must be changed to maintain the inequality $e_1 > e_2 > e_3$. We write

$$\begin{aligned} e_1 &= U_1, \\ e_2 &= \frac{1}{2}[1 - U_1 + (1 + 2U_1 - 3U_1^2)^{1/2}], \\ e_3 &= \frac{1}{2}[1 - U_1 - (1 + 2U_1 - 3U_1^2)^{1/2}]. \end{aligned} \quad (85)$$

We consider the region $U > e_1 > e_2 > e_3$, and write eq.(77) as

$$\left(\frac{dU}{d\phi}\right)^2 = (U - e_1)(U - e_2)(U - e_3). \quad (86)$$

Equation (86) can be integrated [7] with ϕ expressed in terms of an inverse sn function. After some rearrangement, we find

$$\frac{1}{q} = \frac{e_1 - e_2 sn^2(\gamma\phi, k)}{cn^2(\gamma\phi, k)}, \quad (87)$$

where γ and k^2 are calculated using the same expressions given by eq.(81) but with e_1, e_2, e_3 given by eq.(85).

The expressions for e_1, e_2, e_3 given by eqs.(78) and (85) coincide at $k^2 = 1$ for which $e_1 = e_2 = 2/3, e_3 = -1/3$, and both equations (80) and (87) give $U = 2/3$ or $r = 3GM/c^2$ independent of ϕ .

Eq.(87) gives a trajectory of light which terminates at the blackhole when $\phi = \phi_2 = K(k)/\gamma$. As in our discussion of the terminating orbits for the planet, the terminating light ray trajectories can be characterized by the angle ϕ_2 with which the light beam enters the center of the blackhole.

As U_1 increases from $2/3$ to 1 , k^2 covers the entire range $1 \geq k^2 \geq 0$; it decreases from 1 to 0 . When $U_1 = 1$, i.e. when the light beam grazes the Schwarzschild horizon, $e_1 = 1, e_2 = e_3 = 0, k^2 = 0, \gamma = 1/2$, and we have the trajectory of light given by

$$\frac{1}{q} = \frac{1}{\cos^2(\phi/2)}, \quad (88)$$

which gives, for $\phi = 0, U = 1$ or $r = \alpha$, and for $\phi = \pi, U = \infty$ or $r = 0$, i.e. the light is absorbed at the center of the blackhole. Examples of the trajectories of light obtained from eqs.(87) and (88) for $U_1 = 5/6 = 0.83333$ ($R = 2.4GM/c^2$) and 1 ($R = 2GM/c^2$) in Region II are shown as the solid lines in Fig.10 (a) and (b). The path that emerges from the center of the blackhole when ϕ is continued beyond ϕ_2 (shown as a dotted line in Fig.10) again may be interesting if the concept of whitehole is of any physical relevance.

When the distance R to the blackhole at $\phi = 0$ is inside the Schwarzschild horizon, the terminating path takes on a somewhat different form as we show below.

Region II': $1 < U_1 \leq \infty$, or $2GM/c^2 > R \geq 0$

Here R has the same meaning as that in Region II. As U_1 increases beyond 1 , i.e. when R is less than the Schwarzschild radius, e_1 in eq.(85) remains real while e_2 and e_3 become complex. We now write the three roots of the cubic equation $U^3 - U^2 - U_1^3 + U_1^2 = 0$ as a, b and \bar{b} given by

$$\begin{aligned} a &= U_1, \\ b &= \frac{1}{2}[1 - U_1 + i(3U_1^2 - 2U_1 - 1)^{1/2}], \\ \bar{b} &= \frac{1}{2}[1 - U_1 - i(3U_1^2 - 2U_1 - 1)^{1/2}]. \end{aligned} \quad (89)$$

We consider the region $U > a$, and write eq.(77) as

$$\left(\frac{dU}{d\phi}\right)^2 = (U - a)(U - b)(U - \bar{b}). \quad (90)$$

This equation can be integrated [7] with ϕ expressed in terms of an inverse cn function. After a little algebra, we find

$$\frac{1}{q} = \frac{\gamma^2 + a - (\gamma^2 - a)cn(\gamma\phi, k)}{1 + cn(\gamma\phi, k)}, \quad (91)$$

where

$$\gamma = [U_1(3U_1 - 2)]^{1/4} \quad (92)$$

and

$$k^2 = \frac{1}{2} - \frac{3U_1 - 1}{4\sqrt{U_1(3U_1 - 2)}} = \frac{1}{2} - \frac{3a - 1}{4\gamma^2}. \quad (93)$$

Equation (91) gives the trajectory of light when R is inside the Schwarzschild horizon and it terminates at the blackhole when $\phi = \phi_{2'} = 2K(k)/\gamma$, where k and γ are given by eqs.(93) and (92). On the boundary with Region II where $U_1 = 1$, and $k^2 = 0$, $\gamma = 1$ from eqs.(93) and (92), eq.(91) becomes eq.(88) and thus there is no discontinuity in the orbit as it makes a transition from Region II to Region II' across $U_1 = 1$.

We note that as in the case of Region II' for the planetary orbits, Region II' for light trajectories covers a semi-infinite range of the parameter characterizing it ($1 < U_1 \leq \infty$) but is of relevance only to a very small physical region $2GM/c^2 > R \geq 0$ for the initial position of a light beam inside the Schwarzschild horizon. The terminating orbits of light rays in Region II' are also of very little variety as $\phi_{2'}$ is restricted to a limited range of $0 \leq \phi_{2'} \leq \pi$. An example of a terminating trajectory obtained from eq.(91) is shown as the solid line in Fig.10(c) for $U_1 = 10$ ($R = 0.2GM/c^2$); the dotted line again represents a trajectory of light coming out from the center of the blackhole as ϕ is continued beyond $\phi_{2'}$. It may be of some mathematical interest to note that as $U_1 \rightarrow \infty$ or $R \rightarrow 0$, the squared modulus of the Jacobian elliptic functions used to describe the trajectories k^2 approaches a value $(2 - \sqrt{3})/4 = 0.0669873$ that is the same as that given in Section 5 for the case of Region II' for the planetary orbits. Thus the squared modulus of the elliptic functions that describe the terminating light trajectories in Region II' is restricted to a very small range $0 < k^2 \leq 0.0669873$ even as Region II' consists of a very large interval $1 < U_1 \leq \infty$.

8 Summary

We have presented exact analytic expressions given by eqs.(20), (29) and (36) for the planetary orbits in the Schwarzschild geometry. The equations relate the distance r of the planet from the star or blackhole to the polar angle ϕ and are described explicitly by Jacobian elliptic functions of modulus k . Equation (20) gives periodic orbits that describe a planet precessing around a star or blackhole, while eqs.(29) and (36) give terminating orbits that describe a planet plunging into the center of a blackhole. One of the most important aspects of our analysis

is the construction of a map with coordinates (e, s) that we use to view all possible orbits in their entirety, where the two dimensionless parameters e and s are defined by eqs.(11) and (12) which we call the energy and field parameters respectively. For $0 \leq e \leq 1$, we show that there are three regions which we call Regions I ($0 \leq s \leq s_1$), II ($s_1 < s \leq s_2$) and II' ($s_2 < s \leq \infty$) where these orbits are applicable, and where s_1 and s_2 that depend on e are given by eqs.(40) and (57) respectively (Fig.2). Region I has periodic and terminating orbits given by eqs.(20) and (29). Regions II and II' have terminating orbits only given by eq.(36). We have divided Region I into grids that consist of lines of constant precession angle $0 \leq \Delta\phi \leq \infty$ given by eq.(25) and lines of constant true eccentricity $0 \leq \varepsilon \leq 1$ defined by eq.(28) (Fig.3); the lines of constant $\Delta\phi$ are obtained from solving eqs.(38) and (99), and those of constant ε from solving eqs.(38) and (100). These grids make the identification of all possible periodic orbits, including the unbounded and asymptotic ones, convenient and precise. Numerous numerical results for orbits in Region I are presented in Tables 1-6, and examples of precessing orbits, including the unbounded ones, are shown in Figs.4 and 5. Among the interesting results, for example, Table 6 for $\Delta\phi = 2\pi$, $e = 1$, $s = 0.248804$ and Fig.4 f3 show that a planet coming from infinity at zero polar angle, makes a complete loop about the blackhole, and returns to infinity with a polar angle that approaches 2π . Figure 3, or a more refined version of it that can be constructed using the expressions for $\Delta\phi$ and ε that we presented, can be fruitfully used with the experimental observation data. As for the terminating orbits, our orbit equations assume the planet's initial trajectory to be perpendicular to the line joining it to the star or blackhole. The terminating orbits of Region I require the planet to be at a distance $q_1 < 2$ from the star or blackhole, and those of Region II' requires $q_2' \leq 1$, i.e. they require the planet to be initially very close to the blackhole or within the Schwarzschild horizon. The terminating orbits of Region II, on the other hand, are more interesting as the planet can be initially at a distance $1 < q_2 \leq \infty$. We have shown how the periodic orbits of Region I become the asymptotic periodic orbits as $s \rightarrow s_1$, and then become terminating orbits as s becomes greater than s_1 . It is interesting to note that a planet initially at infinity with $e = 1$ and in a trajectory perpendicular to the line joining it to a blackhole can be absorbed by the blackhole if s is greater than 0.25.

We have also presented exact analytic expressions given by eqs.(80), (87) and (91) for the trajectories of light in the presence of a star or blackhole depending on the value of one parameter U_1 that has a range which can be divided into three regions: Regions I ($0 \leq U_1 \leq 2/3$), II ($2/3 < U_1 \leq 1$) and II' ($1 < U_1 \leq \infty$), where U_1 is defined by eq.(76). In Region I, the deflection of light can range from small angles to going continuously around the star or blackhole in a circle. In Regions II and II', light is absorbed into the center of the blackhole. Among the interesting results, a deflection of light by 180° requires a distance of closest approach R to the blackhole equal to $3.5206GM/c^2$ (Fig.9b), and for $R < 3GM/c^2$, light will be absorbed by the blackhole.

We have thus presented a complete map that can help to identify characteristics of stars and blackholes (that are not spinning too fast) from the observed

characteristics of objects or light beams that are affected by them.

9 References

*Electronic address: fhioe@sjfc.edu

[1] M.P. Hobson, G. Efstathiou and A.N. Lasenby: General Relativity, Cambridge University Press, 2006, Chapters 9 and 10.

[2] E.T. Whittaker: A Treatise on the Analytical Dynamics of Particles and Rigid Bodies, 4th Edition, Dover, New York, 1944, Chapter XV.

[3] Y. Hagihara, Japanese Journal of Astronomy and Geophysics VIII, 67 (1931).

[4] S. Chandrasekhar: The Mathematical Theory of Black Holes, Oxford University Press, 1983, Chapter 3.

[5] J. Levin and G. Perez-Giz, Phys. Rev. D 77, 103005 (2008).

[6] F.T. Hioe, Phys. Lett. A 373, 1506 (2009).

[7] P.F. Byrd and M.D. Friedman: Handbook of Elliptic Integrals for Engineers and Scientists, 2nd Edition, Springer-Verlag, New York, 1971. See in particular p.72, 74, 81, 86 for the formulas used in this paper.

[8] See e.g. J. L. Martin: General Relativity: A Guide to its Consequences for Gravity and Cosmology, Ellis Horwood Ltd., Chichester,1988, Chapter 4.

[9] S.V. Iyer and A.O. Petters, Gen. Relat. and Grav. 39, 1563 (2007), C.R. Keeton and A.O. Petters, Phys. Rev. D 72, 104006 (2005).

10 Appendix A Relation Among s, e and k^2

In this Appendix, we derive the relation among s, e and k^2 given by eqs.(38) and (39). Substituting eq.(23) into eq.(22) and after a little algebra, we find

$$\tan \frac{\theta}{3} = \frac{\sqrt{3}k^2}{2 - k^2}, \quad (94)$$

and hence we find

$$\sin \frac{\theta}{3} = \frac{\sqrt{3}k^2}{2\sqrt{1 - k^2 + k^4}}, \quad (95)$$

$$\cos \frac{\theta}{3} = \frac{2 - k^2}{2\sqrt{1 - k^2 + k^4}}. \quad (96)$$

We then find

$$\begin{aligned} \cos \left(\frac{\theta}{3} + \frac{4\pi}{3} \right) &= \frac{-1 + 2k^2}{2\sqrt{1 - k^2 + k^4}}, \\ \cos \left(\frac{\theta}{3} + \frac{2\pi}{3} \right) &= \frac{-1 - k^2}{2\sqrt{1 - k^2 + k^4}}. \end{aligned} \quad (97)$$

Equations (96)-(98) and (23) allow e_1, e_2, e_3 to be expressed in terms of g_2 and k^2 as

$$\begin{aligned} e_1 &= \sqrt{\frac{g_2}{12} \frac{2 - k^2}{\sqrt{1 - k^2 + k^4}}}, \\ e_2 &= \sqrt{\frac{g_2}{12} \frac{-1 + 2k^2}{\sqrt{1 - k^2 + k^4}}}, \\ e_3 &= \sqrt{\frac{g_2}{12} \frac{-1 - k^2}{\sqrt{1 - k^2 + k^4}}}. \end{aligned} \quad (98)$$

Substituting eq.(96) into the relation $\cos \theta = -3 \cos(\theta/3) + 4 \cos^3(\theta/3)$, and substituting the result into eq.(24) gives the relation among s, e and k^2 given by eqs.(38) and (39). For $k^2 = 1$, we get $\cos \theta = -1$ from eqs.(38) and (39), and from eq.(98) we get $e_1 = e_2 = \sqrt{g_2/12} = -(1/2)e_3$.

From eqs.(25), (21), (98) and (10), we find an expression for the precession angle $\Delta\phi$ given by eq.(25) in terms of k and s to be

$$\Delta\phi = 4K(k) \left(\frac{1 - k^2 + k^4}{1 - 12s^2} \right)^{1/4} - 2\pi. \quad (99)$$

11 Appendix B The Energy Parameter e and the True Eccentricity ε in Region I

In this Appendix, we show the relation between the energy parameter e and the true eccentricity ε . The energy parameter e in all three regions I, II and II' is defined by eq.(11). The general or true eccentricity ε is defined by eq.(28). From eq.(28), (26) and (27) and using the expressions (98) of e_1, e_2, e_3 in terms of k^2 given in Appendix A, we find that ε can be expressed as

$$\varepsilon = \frac{6(e_2 - e_3)}{1 + 6(e_2 + e_3)}$$

or

$$\varepsilon = \frac{3k^2\sqrt{1 - 12s^2}}{2\sqrt{1 - k^2 + k^4} - (2 - k^2)\sqrt{1 - 12s^2}}. \quad (100)$$

For small s^2 and k^2 , we find that

$$\varepsilon \simeq \frac{3k^2/2}{1 - (1 - 6s^2)} \simeq \frac{k^2}{4s^2} \simeq e \quad (101)$$

because $k^2 \simeq 4es^2$ for very small k^2 and s^2 [6]. We thus confirm the identification of e defined in eq.(11) with the eccentricity of the orbit in Newtonian mechanics. As we pointed out in the text, ε is generally not equal to e . However, as we show below, $\varepsilon = e$ exactly when $e = 1$ and in this case the orbits are unbounded.

For the possibility of unbounded orbits in Region I, we set the initial $q = \infty$ at $\phi = 0$ in eq.(20), and get

$$\frac{1}{3} + 4e_3 = 0, \quad (102)$$

or

$$e_3 = -\frac{1}{12}. \quad (103)$$

Using eqs.(23), (10) and (97) that give e_3 in terms of s and k^2 , and after a little algebra, we find the simple equation that relates s to k^2 on $e = 1$ to be given by eq.(51).

This simple equation (51) between s and k^2 for $e = 1$ can be used for any $0 \leq k^2 \leq 1$. For example, we find that for $k^2 = 1$, $s = 1/4 = 0.25$, and for $k^2 = 1/2$, $s = 1/(3\sqrt{2}) = 0.235702$. For $e = 1$, and for small k^2 , we have $s^2 \simeq k^2/4$ which is a special case of $k^2 \simeq 4es^2$ that is valid more generally for $0 \leq e \leq 1$.

In addition, we find $g_2 = 1/12 - s^2 = 1/12 - k^2/[4(1 + k^2)^2]$ and therefore

$$g_2 = \frac{1 - k^2 + k^4}{12(1 + k^2)^2}, \quad (104)$$

and from the expression for e_1 and e_2 given by eq.(98), we find

$$\begin{aligned} e_1 &= \frac{2 - k^2}{12(1 + k^2)}, \\ e_2 &= \frac{-1 + 2k^2}{12(1 + k^2)}. \end{aligned} \quad (105)$$

Thus from the expressions (27), (30), and (21) for q_{\min} , q_1 , and γ , we find that when $e = 1$, they have the simple expressions given by eqs.(53), (54) and (52).

Also, substituting eq.(48) into eq.(100) shows that $\varepsilon = 1$ when $e = 1$, i.e. ε and e coincide at $e = 1$.

12 Appendix C Some Simple Relations for the Special Case of $k^2 = 1/2$

It is known that in elliptic functions, the squared modulus $k^2 = 1/2$ is a special value for which many simple relations arise. We first consider the case of $k^2 = 1/2$ in Region I. We note that substituting $k^2 = 1/2$ into eq.(22) gives a relation $e_1 + e_3 = 2e_2$, and substituting the expressions of e_1, e_2, e_3 from eq.(23) into this relation gives $\theta/3 = \pi/6$, or $\theta = \pi/2$. Thus $\cos \theta = 0$ which results in

$$g_3 = 0 \quad (106)$$

from eq.(24), which in turn gives a simple relationship

$$s^2 = \frac{1}{6(1-e^2)} \left(1 - \sqrt{\frac{1+2e^2}{3}} \right). \quad (107)$$

For example, we have $s = \sqrt{(3-\sqrt{3})/18} = 0.265408$ for $e = 0$, and $s = 1/(3\sqrt{2}) = 0.235702$ for $e = 1$ (using L'Hospital rule). These two values represent the two terminal coordinates of the constant $k^2 = 1/2$ line in Region I (see Fig.1). The other solution of eq.(106) is eq.(58) which is applicable for Region II as we shall show later in this Appendix.

We also find from eq.(23) that

$$\begin{aligned} e_1 &= -e_3 = \frac{\sqrt{g_2}}{2}, \\ e_2 &= 0, \end{aligned} \quad (108)$$

and

$$\gamma = \sqrt[4]{g_2}, \quad (109)$$

and the orbit equation (20) becomes

$$\frac{1}{q} = \frac{1}{3} - 2\sqrt{g_2}cn^2(\gamma\phi, 1/\sqrt{2}),$$

where the s value for g_2 in this case is given by eq.(107) for Region I. The precession angle $\Delta\phi$ can be found from eq.(25) and from $K(1/\sqrt{2}) = 1.85407$. It is given by

$$\frac{\Delta\phi}{\pi} = \frac{1.18034}{\sqrt[4]{g_2}} - 2.$$

From eqs.(26)-(28) and (108), we find

$$\varepsilon = \frac{6(e_2 - e_3)}{1 + 6(e_2 + e_3)} = \frac{3\sqrt{g_2}}{1 - 3\sqrt{g_2}}, \quad (110)$$

which can be inverted and solved for s in terms of ε , giving

$$s^2 = \frac{3 + 6\varepsilon - \varepsilon^2}{36(1 + \varepsilon)^2}. \quad (111)$$

Substituting eq.(111) into eq.(106) gives e in terms of ε as

$$e^2 = 1 - \frac{12(1 + \varepsilon)^2(1 - \varepsilon)(1 + 3\varepsilon)}{(3 + 6\varepsilon - \varepsilon^2)^2}. \quad (112)$$

Since for $e = 0$, $s = \sqrt{(3-\sqrt{3})/18}$ when $k^2 = 1/2$ as we showed above, substituting this s value into eq.(106) gives $\varepsilon = (2/\sqrt{-3 + 2\sqrt{3}} - 1)^{-1} = 0.516588$.

For $e = 1$, $s = 1/(3\sqrt{2})$ when $k^2 = 1/2$, and substituting this s value into eq.(106) gives $\varepsilon = 1$ as it should. Thus eqs.(111) and (112) are the parametric equations for the line of constant $k^2 = 1/2$ which can be used instead of eq.(107) as ε takes the values between 0.516588 and 1.

Also, substituting $e_2 = 0$ from eq.(108) into eq.(27) gives

$$q_{\min} = 3 \quad (113)$$

independent of e for $k^2 = 1/2$, as shown in Table 3.

We now consider $k^2 = 1/2$ in Region II. From eqs.(35) and (33), we have

$$a = A + B = 0. \quad (114)$$

From eq.(32), and from $A = -B$, and $A^3 = -B^3$, we arrive again at eq.(106) with the same g_3 given by eq.(10). This explains why we stated after eq.(107) that the other solution of eq.(106) given by eq.(58) gives the relation between s and e for Region II. The two equations (108) and (58) that give simple relations between s and e in two different regions and that arise as two different solutions of the same equation (106) show a rather remarkable symmetry exhibited by the special case $k^2 = 1/2$.

It also follows from eqs.(32) and (34) that

$$A = \frac{1}{2} \left(\frac{-g_2}{3} \right)^{1/2} = \frac{1}{12} \sqrt{12s^2 - 1}, \quad (115)$$

$$\gamma = (3A^2)^{1/4} = \frac{1}{2} \left[\frac{1}{3} (12s^2 - 1) \right]^{1/4}, \quad (116)$$

and that the orbit equation (36) becomes

$$\frac{1}{q} = \frac{1}{3} + 4\gamma^2 \frac{1 - cn(2\gamma\phi, 1/\sqrt{2})}{1 + cn(2\gamma\phi, 1/\sqrt{2})}, \quad (117)$$

where the s value for the above equations is given by eq.(58) for $0 \leq e \leq 1$.

Since $a = 0$, the initial distance q_2 of the planet from the blackhole is $q_2 = 3$ from eq.(37), independent of e , as shown in Table 10.

13 Appendix D The Boundaries of Region II

On the upper boundary $s_2^2 = 1/(1 - e^2)$ of Region II, the planet starts from the Schwarzschild horizon given by $q = 1$, which implies that for $\phi = 0$, $1/q = 1/3 + 4a$ from eq.(36), or

$$1 = \frac{1}{3} + 4a. \quad (118)$$

Hence

$$a = A + B = \frac{1}{6}. \quad (119)$$

Since from eqs.(32) and (17),

$$AB = \frac{1}{4} \left(g_3^2 - \frac{\Delta}{27} \right)^{1/3} = \frac{g_2}{12}, \quad (120)$$

we can conclude from eqs.(35) and (34) that k^2 and γ are given on the boundary $s_2^2 = 1/(1 - e^2)$ of Region II by eqs.(60) and (61).

In particular, for $e = 0$, $s = 1$, we find $\gamma = (5/16)^{1/4} = 0.747674$, $k^2 = (1 - 1/\sqrt{5})/2 = 0.276393$, and this is the minimum value of k^2 in Region II.

We now consider the right boundary $e = 1$ of Region II. Consider the unbounded orbit of a planet coming from infinity that requires, from eq.(36), that

$$\frac{1}{3} + 4a = 0, \quad (121)$$

or

$$a = -\frac{1}{12}. \quad (122)$$

From

$$A + B = a = -\frac{1}{12}, \quad (123)$$

and

$$AB = \frac{g_2}{12}, \quad (124)$$

and from eqs.(34) and (35), we find eqs.(62) and (64) that give k^2 and γ in terms of s on the boundary $e = 1$ of Region II.

Finally, there is a special case of $g_2 = 0$ or $s^2 = 1/12$ ($s = 1/2\sqrt{3} = 0.288675135$) in Region II that is somewhat interesting. If g_2 of eq.(10) is equal to zero, then $\Delta = 27g_3^2$ from eq.(17), and from eqs.(32)-(35), we find $A = (2g_3)^{1/3}/2$, $B = 0$, $a = A$, $\gamma = (3A^2)^{1/4}$, and noting that $A < 0$ for $s^2 = 1/12$ and $0 \leq e \leq 1$, we have

$$k^2 = \frac{1}{2} - \frac{\sqrt{3}A}{4|A|} = \frac{1}{2} + \frac{\sqrt{3}}{4} = 0.933012702$$

which is independent of e , i.e. the constant $k^2 = (2 + \sqrt{3})/4$ curve in Region II just above the boundary curve of Regions I and II in Fig.2 is a horizontal line. Thus the terminating orbits represented by eq.(36) for any point along this horizontal line are represented by elliptic functions of the same squared modulus given above. It should be remembered, however, that the orbits and the initial positions of the planet (the initial trajectory of which is perpendicular to the

line joining it to the blackhole) depend also on γ and a that are dependent on the value of e . Thus the orbit for $e = 1$, for example, that gives $a = -1/12$ (and $\gamma = 1/(2 \cdot 3^{1/4}) = 0.379917843$) is a terminating orbit for a planet that is initially infinitely far away from a blackhole.

Table 1: Values of s for various values of e and k^2 in Region I

s	$e = 0.0$	$e = 0.1$	$e = 0.2$	$e = 0.3$	$e = 0.4$	$e = 0.5$	$e = 0.6$	$e = 0.7$	$e = 0.8$	$e = 0.9$	$e = 1.0$
$k^2 = 0.001$	0.0554787	0.0454170	0.0346617	0.0286392	0.0248892	0.0222952	0.0203686	0.0188667	0.0176539	0.0166480	0.0157963
$k^2 = 0.01$	0.114809	0.109191	0.0969713	0.0851063	0.0757980	0.0686999	0.0631762	0.0587575	0.0551328	0.0520954	0.0495050
$k^2 = 0.1$	0.210213	0.208385	0.203281	0.195887	0.187374	0.178683	0.170376	0.162703	0.155729	0.149428	0.143740
$k^2 = 0.2$	0.238703	0.237612	0.234488	0.229734	0.223875	0.217424	0.210787	0.204236	0.197932	0.191956	0.186339
$k^2 = 0.3$	0.252575	0.251809	0.249595	0.246160	0.241814	0.236873	0.231612	0.226239	0.220900	0.215689	0.210663
$k^2 = 0.4$	0.260533	0.259944	0.258236	0.255562	0.252131	0.248163	0.243857	0.239372	0.234829	0.230311	0.225877
$k^2 = 0.5$	0.265408	0.264926	0.263523	0.261314	0.258458	0.255122	0.251460	0.247600	0.243642	0.239658	0.235702
$k^2 = 0.6$	0.268462	0.268045	0.266831	0.264913	0.262422	0.259494	0.256258	0.252821	0.249269	0.245666	0.242061
$k^2 = 0.7$	0.270350	0.269973	0.268875	0.267137	0.264873	0.262203	0.259239	0.256076	0.252791	0.249443	0.246076
$k^2 = 0.8$	0.271452	0.271099	0.270069	0.268436	0.266305	0.263787	0.260985	0.257986	0.254863	0.251671	0.248452
$k^2 = 0.9$	0.272006	0.271665	0.270668	0.269088	0.267025	0.264583	0.261863	0.258948	0.255908	0.252796	0.249653
$k^2 = 1.0$	0.272166	0.271828	0.270840	0.269276	0.267232	0.264812	0.262116	0.259225	0.256209	0.253120	0.250000

Table 2: Values of q_{\max} for various values of e and k^2 in Region I

q_{\max}	$e = 0.0$	$e = 0.1$	$e = 0.2$	$e = 0.3$	$e = 0.4$	$e = 0.5$	$e = 0.6$	$e = 0.7$	$e = 0.8$	$e = 0.9$	$e = 1.0$
$k^2 = 0.001$	174.74	273.42	522.17	871.99	1345.9	2012.0	3012.8	4681.4	8018.4	18025	∞
$k^2 = 0.01$	43.673	49.688	68.266	99.742	145.78	212.38	313.52	482.96	822.60	1842.4	∞
$k^2 = 0.1$	14.306	14.851	16.550	19.608	24.429	31.802	43.389	63.171	103.21	223.98	∞
$k^2 = 0.2$	11.377	11.697	12.693	14.481	17.300	21.627	28.458	40.168	63.938	135.75	∞
$k^2 = 0.3$	10.282	10.534	11.314	12.713	14.914	18.291	23.625	32.774	51.357	107.53	∞
$k^2 = 0.4$	9.7280	9.9479	10.630	11.849	13.766	16.704	21.342	29.298	45.460	94.318	∞
$k^2 = 0.5$	9.4118	9.6145	10.243	11.365	13.128	15.828	20.089	27.397	42.239	87.109	∞
$k^2 = 0.6$	9.2220	9.4148	10.012	11.078	12.751	15.314	19.356	26.285	40.359	82.903	∞
$k^2 = 0.7$	9.1078	9.2946	9.8733	10.906	12.527	15.008	18.920	25.627	39.246	80.413	∞
$k^2 = 0.8$	9.0421	9.2256	9.7938	10.808	12.399	14.833	18.672	25.252	38.612	78.997	∞
$k^2 = 0.9$	9.0094	9.1912	9.7542	10.759	12.335	14.747	18.549	25.066	38.299	78.296	∞
$k^2 = 1.0$	9.0000	9.1814	9.7429	10.745	12.317	14.722	18.514	25.013	38.209	78.095	∞

Table 3: Values of q_{\min} for various values of e and k^2 in Region I

q_{\min}	$e = 0.0$	$e = 0.1$	$e = 0.2$	$e = 0.3$	$e = 0.4$	$e = 0.5$	$e = 0.6$	$e = 0.7$	$e = 0.8$	$e = 0.9$	$e = 1.0$
$k^2 = 0.001$	149.15	215.27	343.84	466.77	574.79	669.11	751.92	825.10	890.20	948.48	1001.0
$k^2 = 0.01$	31.135	33.980	41.469	50.945	60.399	69.110	76.948	83.963	90.248	95.899	101.00
$k^2 = 0.1$	7.0549	7.1489	7.4154	7.8125	8.2864	8.7891	9.2876	9.7635	10.209	10.621	11.000
$k^2 = 0.2$	4.7480	4.7753	4.8530	4.9703	5.1133	5.2691	5.4278	5.5830	5.7311	5.8703	6.0000
$k^2 = 0.3$	3.8359	3.8465	3.8765	3.9220	3.9777	4.0389	4.1018	4.1639	4.2237	4.2803	4.3333
$k^2 = 0.4$	3.3289	3.3325	3.3428	3.3583	3.3773	3.3983	3.4199	3.4413	3.4619	3.4815	3.5000
$k^2 = 0.5$	3.0000	3.0000	3.0000	3.0000	3.0000	3.0000	3.0000	3.0000	3.0000	3.0000	3.0000
$k^2 = 0.6$	2.7667	2.7645	2.7585	2.7494	2.7382	2.7260	2.7134	2.7009	2.6889	2.6774	2.6667
$k^2 = 0.7$	2.5911	2.5877	2.5778	2.5629	2.5446	2.5247	2.5042	2.4840	2.4645	2.4460	2.4286
$k^2 = 0.8$	2.4535	2.4491	2.4366	2.4178	2.3949	2.3698	2.3442	2.3189	2.2946	2.2716	2.2500
$k^2 = 0.9$	2.3422	2.3371	2.3228	2.3012	2.2751	2.2465	2.2174	2.1887	2.1613	2.1354	2.1111
$k^2 = 1.0$	2.2500	2.2445	2.2288	2.2052	2.1767	2.1458	2.1142	2.0833	2.0538	2.0259	2.0000

Table 4: Values of $\Delta\phi/\pi$ for various values of e and k^2 in Region I

$\Delta\phi/\pi$	$e = 0.0$	$e = 0.1$	$e = 0.2$	$e = 0.3$	$e = 0.4$	$e = 0.5$	$e = 0.6$	$e = 0.7$	$e = 0.8$	$e = 0.9$	$e = 1.0$
$k^2 = 0.001$	0.018906	0.012572	0.0072747	0.0049522	0.0037347	0.0029941	0.0024975	0.0021419	0.0018748	0.0016669	0.0015004
$k^2 = 0.01$	0.088019	0.078760	0.060819	0.046033	0.036087	0.029413	0.024739	0.021316	0.018713	0.016671	0.015029
$k^2 = 0.1$	0.42211	0.41041	0.37969	0.33964	0.29902	0.26259	0.23177	0.20625	0.18522	0.16780	0.15323
$k^2 = 0.2$	0.69762	0.68449	0.64888	0.59968	0.54604	0.49423	0.44737	0.40639	0.37108	0.34079	0.31478
$k^2 = 0.3$	0.95650	0.94206	0.90245	0.84652	0.78377	0.72123	0.66290	0.61042	0.56410	0.52353	0.48808
$k^2 = 0.4$	1.2200	1.2043	1.1608	1.0987	1.0281	0.95649	0.88857	0.82648	0.77085	0.72150	0.67786
$k^2 = 0.5$	1.5029	1.4858	1.4383	1.3701	1.2917	1.2116	1.1348	1.0638	0.99972	0.94234	0.89123
$k^2 = 0.6$	1.8226	1.8038	1.7519	1.6770	1.5905	1.5015	1.4157	1.3360	1.2635	1.1982	1.1398
$k^2 = 0.7$	2.2072	2.1866	2.1293	2.0465	1.9507	1.8517	1.7559	1.6666	1.5851	1.5114	1.4453
$k^2 = 0.8$	2.7169	2.6938	2.6295	2.5365	2.4286	2.3170	2.2087	2.1075	2.0150	1.9312	1.8558
$k^2 = 0.9$	3.5401	3.5129	3.4374	3.3281	3.2011	3.0696	2.9419	2.8224	2.7130	2.6139	2.5247
$k^2 = 1.0$	∞	∞	∞	∞	∞	∞	∞	∞	∞	∞	∞

Table 5: Values of ϵ for various values of e and k^2 in Region I

ϵ	$e = 0.0$	$e = 0.1$	$e = 0.2$	$e = 0.3$	$e = 0.4$	$e = 0.5$	$e = 0.6$	$e = 0.7$	$e = 0.8$	$e = 0.9$	$e = 1.0$
$k^2 = 0.001$	0.079005	0.11900	0.20592	0.30268	0.40148	0.50088	0.60054	0.70032	0.80015	0.90002	1
$k^2 = 0.01$	0.16760	0.18774	0.24420	0.32383	0.41413	0.50896	0.60587	0.70380	0.80227	0.90105	1
$k^2 = 0.1$	0.33947	0.35009	0.38115	0.43017	0.49343	0.56695	0.64738	0.73227	0.81998	0.90946	1
$k^2 = 0.2$	0.41109	0.42021	0.44683	0.48894	0.54373	0.60819	0.67964	0.75594	0.83548	0.91710	1
$k^2 = 0.3$	0.45659	0.46503	0.48963	0.52845	0.57889	0.63825	0.70412	0.77454	0.84802	0.92344	1
$k^2 = 0.4$	0.49009	0.49813	0.52152	0.55832	0.60598	0.66190	0.72378	0.78978	0.85847	0.92880	1
$k^2 = 0.5$	0.51659	0.52436	0.54692	0.58231	0.62797	0.68133	0.74014	0.80261	0.86737	0.93341	1
$k^2 = 0.6$	0.53845	0.54603	0.56798	0.60232	0.64644	0.69778	0.75410	0.81364	0.87508	0.93743	1
$k^2 = 0.7$	0.55703	0.56445	0.58594	0.61944	0.66233	0.71200	0.76623	0.82327	0.88183	0.94096	1
$k^2 = 0.8$	0.57314	0.58044	0.60155	0.63437	0.67623	0.72449	0.77692	0.83179	0.88781	0.94410	1
$k^2 = 0.9$	0.58733	0.59454	0.61534	0.64759	0.68857	0.73560	0.78645	0.83939	0.89316	0.94690	1
$k^2 = 1.0$	0.60000	0.60713	0.62766	0.65942	0.69963	0.74558	0.79502	0.84623	0.89798	0.94943	1

Table 6: Values of s for constant values of $\Delta\phi$ in Region I

s	$e = 0.0$	$e = 0.1$	$e = 0.2$	$e = 0.3$	$e = 0.4$	$e = 0.5$	$e = 0.6$	$e = 0.7$	$e = 0.8$	$e = 0.9$	$e = 1.0$
$\Delta\phi = \pi/18$	0.0929975	0.0929922	0.0929763	0.0929498	0.0929129	0.0928655	0.0928078	0.0927400	0.0926622	0.0925745	0.0924773
$\Delta\phi = \pi/6$	0.150971	0.150946	0.150871	0.150747	0.150574	0.150353	0.150087	0.149776	0.149424	0.149031	0.148601
$\Delta\phi = \pi/3$	0.195246	0.195185	0.195000	0.194694	0.194273	0.193741	0.193104	0.192372	0.191551	0.190651	0.189680
$\Delta\phi = \pi/2$	0.220477	0.220377	0.220080	0.219591	0.218920	0.218080	0.217085	0.215951	0.214696	0.213336	0.211888
$\Delta\phi = \pi$	0.254214	0.254018	0.253437	0.252492	0.251216	0.249650	0.247838	0.245823	0.243650	0.241354	0.238971
$\Delta\phi = 3\pi/2$	0.265371	0.265111	0.264346	0.263113	0.261468	0.259478	0.257210	0.254729	0.252091	0.249347	0.246537
$\Delta\phi = 2\pi$	0.269502	0.269206	0.268334	0.266938	0.265091	0.262877	0.260379	0.257671	0.254819	0.251875	0.248804
$\Delta\phi = \infty$	0.272166	0.271828	0.270840	0.269276	0.267232	0.264812	0.262116	0.259225	0.256209	0.253120	0.250000

Table 7: Values of s for constant values of ϵ in Region I

s	$e = 0.00$	$e = 0.02$	$e = 0.04$	$e = 0.06$	$e = 0.08$	$e = 0.10$	$e = 0.12$	$e = 0.14$	$e = 0.16$	$e = 0.18$	$e = 0.20$
$\epsilon = 0.2$	0.135153	0.134536	0.132663	0.129457	0.124776	0.118388	0.109916	0.0987083	0.0835085	0.0611485	0
s	$e = 0.00$	$e = 0.04$	$e = 0.08$	$e = 0.12$	$e = 0.16$	$e = 0.20$	$e = 0.24$	$e = 0.28$	$e = 0.32$	$e = 0.36$	$e = 0.40$
$\epsilon = 0.4$	0.234806	0.234069	0.231803	0.227832	0.221831	0.213264	0.201255	0.184309	0.159570	0.120022	0
s	$e = 0.00$	$e = 0.06$	$e = 0.12$	$e = 0.18$	$e = 0.24$	$e = 0.30$	$e = 0.36$	$e = 0.42$	$e = 0.48$	$e = 0.54$	$e = 0.60$
$\epsilon = 0.6$	0.272166	0.272037	0.271572	0.270524	0.268439	0.264552	0.257565	0.245130	0.222468	0.177299	0
s	$e = 0.61$	$e = 0.62$	$e = 0.64$	$e = 0.66$	$e = 0.68$	$e = 0.70$	$e = 0.72$	$e = 0.74$	$e = 0.76$	$e = 0.78$	$e = 0.80$
$\epsilon = 0.8$	0.261834	0.261450	0.259987	0.257309	0.252931	0.246121	0.235710	0.219699	0.194219	0.149735	0

Table 8: Values of q_1 for various values of e and k^2 in Region I (terminating orbits)

q_1	$e = 0.0$	$e = 0.1$	$e = 0.2$	$e = 0.3$	$e = 0.4$	$e = 0.5$	$e = 0.6$	$e = 0.7$	$e = 0.8$	$e = 0.9$	$e = 1.0$
$k^2 = 0.001$	1.0126	1.0084	1.0048	1.0033	1.0025	1.0020	1.0017	1.0014	1.0012	1.0011	1.0010
$k^2 = 0.01$	1.0582	1.0521	1.0403	1.0306	1.0240	1.0196	1.0165	1.0142	1.0124	1.0111	1.0100
$k^2 = 0.1$	1.2685	1.2614	1.2427	1.2180	1.1928	1.1699	1.1504	1.1341	1.1206	1.1094	1.1000
$k^2 = 0.2$	1.4255	1.4182	1.3983	1.3703	1.3394	1.3089	1.2810	1.2563	1.2348	1.2161	1.2000
$k^2 = 0.3$	1.5575	1.5502	1.5299	1.5007	1.4672	1.4332	1.4008	1.3711	1.3445	1.3209	1.3000
$k^2 = 0.4$	1.6756	1.6683	1.6481	1.6186	1.5841	1.5483	1.5135	1.4809	1.4511	1.4242	1.4000
$k^2 = 0.5$	1.7844	1.7773	1.7574	1.7281	1.6935	1.6570	1.6210	1.5869	1.5552	1.5263	1.5000
$k^2 = 0.6$	1.8864	1.8795	1.8601	1.8315	1.7973	1.7610	1.7248	1.6900	1.6575	1.6275	1.6000
$k^2 = 0.7$	1.9831	1.9764	1.9578	1.9301	1.8968	1.8612	1.8254	1.7908	1.7582	1.7279	1.7000
$k^2 = 0.8$	2.0754	2.0691	2.0513	2.0248	1.9929	1.9584	1.9236	1.8898	1.8577	1.8278	1.8000
$k^2 = 0.9$	2.1642	2.1583	2.1415	2.1164	2.0860	2.0532	2.0198	1.9872	1.9562	1.9271	1.9000
$k^2 = 1.0$	2.2500	2.2445	2.2288	2.2052	2.1767	2.1458	2.1142	2.0833	2.0538	2.0259	2.0000

Table 9: Values of s for various values of e and k^2 in Region II

s	$e = 0.0$	$e = 0.1$	$e = 0.2$	$e = 0.3$	$e = 0.4$	$e = 0.5$	$e = 0.6$	$e = 0.7$	$e = 0.8$	$e = 0.9$	$e = 1.0$
$k^2 = 1.0$	0.272166	0.271828	0.270840	0.269276	0.267232	0.264812	0.262116	0.259225	0.256209	0.253120	0.250000
$k^2 = 0.9$	0.297739	0.297917	0.298442	0.299293	0.300443	0.301865	0.303537	0.305444	0.307575	0.309927	0.312500
$k^2 = 0.8$	0.329945	0.330718	0.333024	0.336843	0.342169	0.349050	0.357613	0.368098	0.380913	0.396727	0.416667
$k^2 = 0.7$	0.371926	0.373406	0.377868	0.385401	0.396232	0.410826	0.430060	0.455531	0.490285	0.540844	0.625000
$k^2 = 0.6$	0.429234	0.431592	0.438767	0.451100	0.469328	0.494871	0.530424	0.581374	0.659978	0.802847	1.25000
$k^2 = 0.5$	0.512730	0.516250	0.527046	0.545908	0.574478	0.615920	0.676462	0.769603	0.930895	1.30267	—
$k^2 = 0.4$	0.646974	0.652192	0.668307	0.696858	0.741019	0.806949	0.907116	1.07001	1.37756	2.21530	—
$k^2 = 0.3$	0.901890	0.910054	0.935412	0.980848	1.05231	—	—	—	—	—	—

Table 10: Values of q_2 for various values of e and k^2 in Region II

q_2	$e = 0.0$	$e = 0.1$	$e = 0.2$	$e = 0.3$	$e = 0.4$	$e = 0.5$	$e = 0.6$	$e = 0.7$	$e = 0.8$	$e = 0.9$	$e = 1.0$
$k^2 = 1.0$	9.0000	9.1814	9.7429	10.745	12.317	14.722	18.514	25.013	38.209	78.095	∞
$k^2 = 0.9$	7.6760	7.7965	8.1685	8.8291	9.8596	11.426	13.833	18.073	26.550	52.109	∞
$k^2 = 0.8$	6.4074	6.4806	6.7060	7.1041	7.7200	8.6471	10.084	12.507	17.353	31.823	∞
$k^2 = 0.7$	5.1997	5.2381	5.3557	5.5620	5.8780	6.3467	7.0597	8.2346	10.522	17.148	∞
$k^2 = 0.6$	4.0606	4.0750	4.1191	4.1959	4.3120	4.4809	4.7310	5.1276	5.8592	7.8120	∞
$k^2 = 0.5$	3.0000	3.0000	3.0000	3.0000	3.0000	3.0000	3.0000	3.0000	3.0000	3.0000	—
$k^2 = 0.4$	2.0324	2.0259	2.0059	1.9717	1.9217	1.8523	1.7574	1.6241	1.4235	1.0692	—
$k^2 = 0.3$	1.1805	1.1733	1.1516	1.1148	1.0618	—	—	—	—	—	—

Table 11: Values of ϕ_2/π for various values of e and k^2 in Region II

ϕ_2/π	$e = 0.0$	$e = 0.1$	$e = 0.2$	$e = 0.3$	$e = 0.4$	$e = 0.5$	$e = 0.6$	$e = 0.7$	$e = 0.8$	$e = 0.9$	$e = 1.0$
$k^2 = 1.0$	∞	∞	∞	∞	∞	∞	∞	∞	∞	∞	∞
$k^2 = 0.9$	2.6599	2.6469	2.6099	2.5551	2.4890	2.4176	2.3448	2.2733	2.2043	2.1385	2.0761
$k^2 = 0.8$	2.1586	2.1480	2.1175	2.0711	2.0132	1.9479	1.8781	1.8055	1.7309	1.6541	1.5742
$k^2 = 0.7$	1.8169	1.8079	1.7819	1.7412	1.6889	1.6274	1.5584	1.4822	1.3977	1.3010	1.1817
$k^2 = 0.6$	1.5360	1.5283	1.5060	1.4703	1.4231	1.3654	1.2977	1.2186	1.1237	1.0002	0.78496
$k^2 = 0.5$	1.2822	1.2758	1.2569	1.2262	1.1843	1.1315	1.0671	0.98815	0.88720	0.74053	—
$k^2 = 0.4$	1.0373	1.0321	1.0166	0.99105	0.95540	0.90923	0.85112	0.77757	0.68006	0.53257	—
$k^2 = 0.3$	0.78606	0.78213	0.77030	0.75047	0.72230	—	—	—	—	—	—

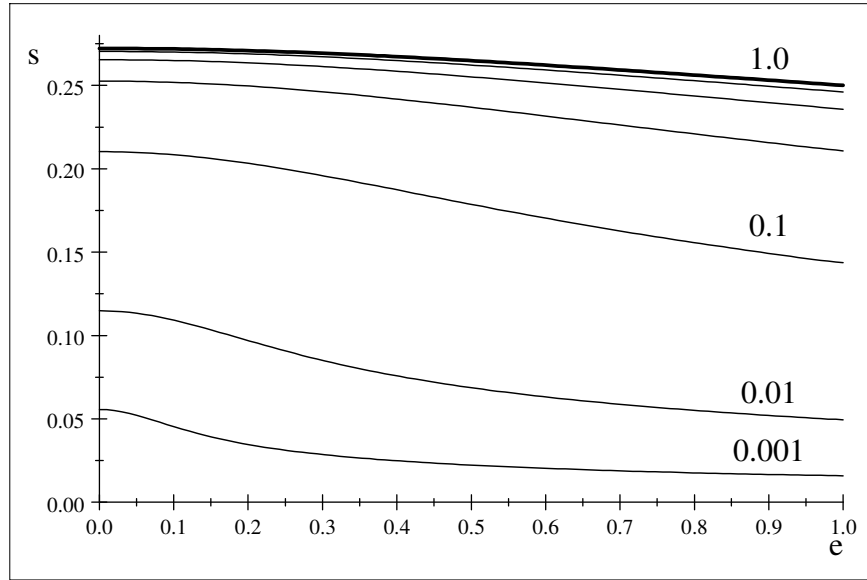


Fig. 1. Region I plots of $k^2 = 0.001, 0.01, 0.1, 0.3, 0.5, 0.7, 1.0$

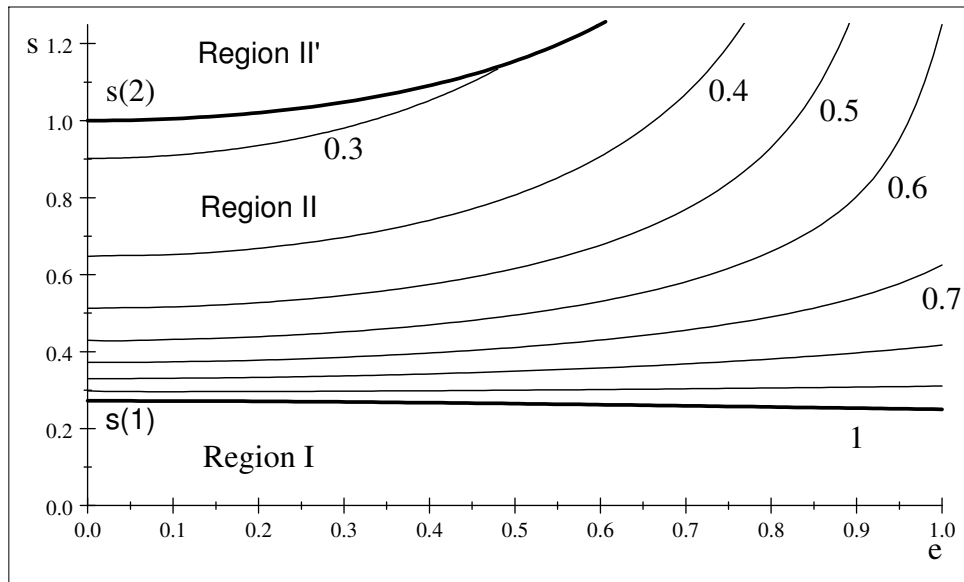


Fig. 2. Region II plots of $k^2 = 1.0, 0.9, 0.8, 0.7, 0.6, 0.5, 0.4, 0.3$

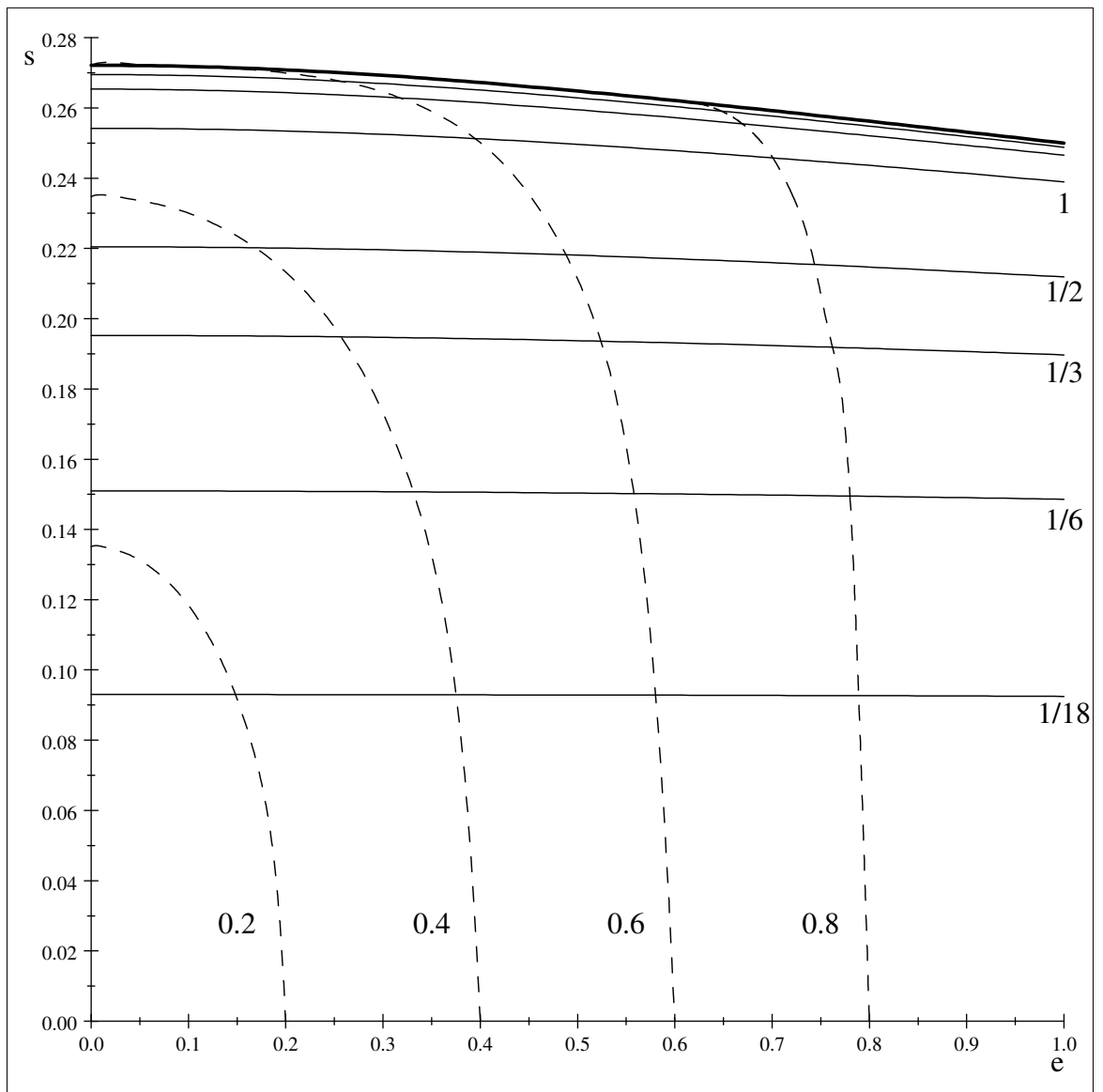


Fig. 3. $\Delta\phi/\pi = 1/18, 1/6, 1/3, 1/2, 1, 3/2, 2$ and $\epsilon = 0.2, 0.4, 0.6, 0.8$ (Region I)

Fig. 4. Region I: Periodic(a1-f1,a2-f2), unbounded(a3-g3), asymptotic periodic orbits(g1-g3) for $\Delta\varphi$ equal to (a) $\pi/6$, (b) $\pi/3$, (c) $\pi/2$, (d) π , (e) $3\pi/2$, (f) 2π , (g) ∞ and for e equal to (1) 0, (2) 0.5, (3) 1.

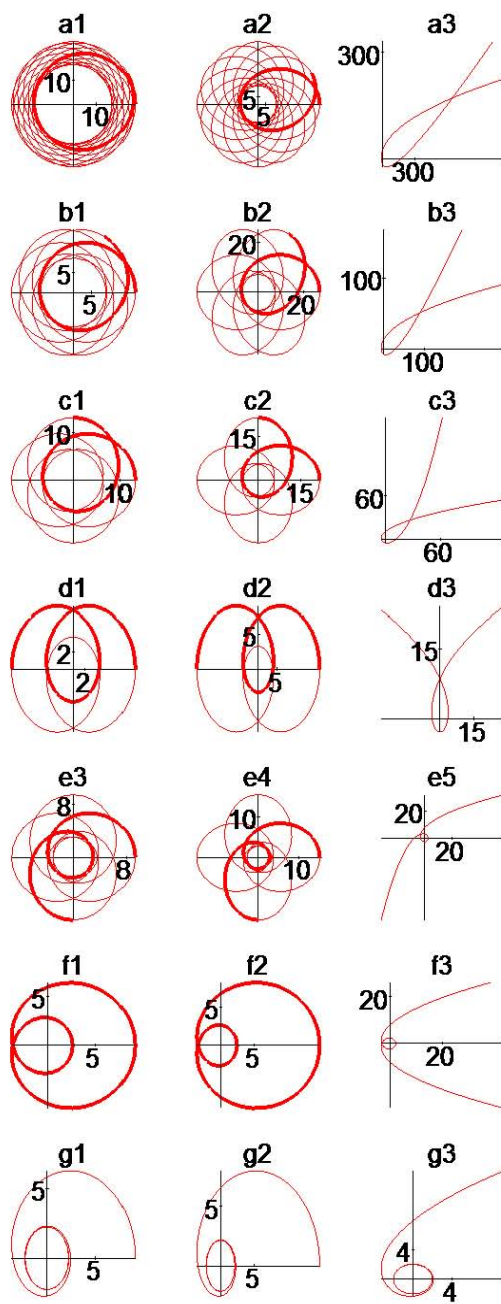


Fig. 5. Precessional orbit for $\Delta\varphi = \left(\frac{1}{3} + 0.002614 \dots\right)\pi$, $\epsilon = 0.58143 \dots$, $e = 0.5$, $s = 0.194229 \dots$

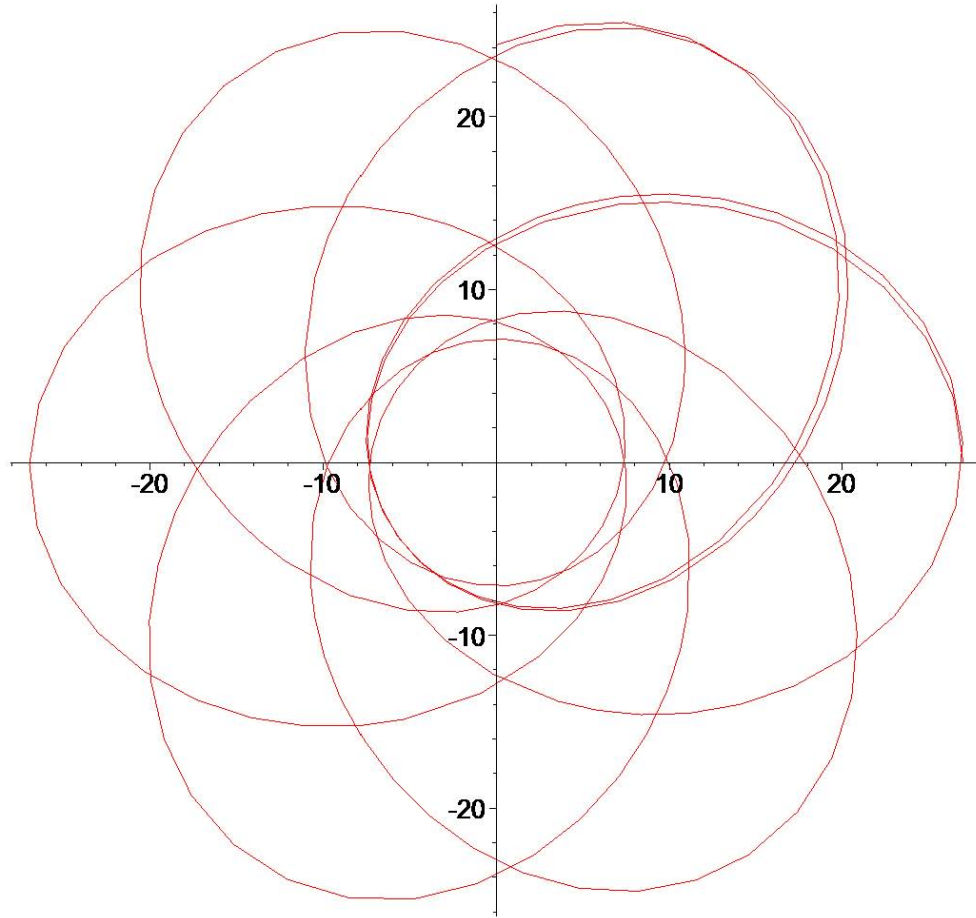


Fig. 6. Terminating orbits in region I

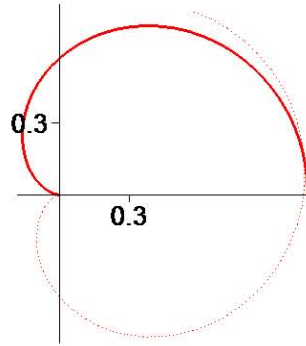
(a) $k^2 = 0.01$, $e = 0$, $s = 0.114809$, $\frac{\varphi_1}{\pi} = 1.0440$, $q_1 = 1.0582$

(b) $k^2 = 0.1$, $e = 0.5$, $s = 0.178683$, $\frac{\varphi_1}{\pi} = 1.1313$, $q_1 = 1.1699$

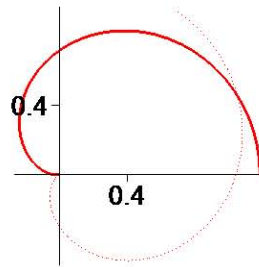
(c) $k^2 = 0.9$, $e = 0.9$, $s = 0.252796$, $\frac{\varphi_1}{\pi} = 2.3070$, $q_1 = 1.9271$

(d) $k^2 = 1$, $e = 1$, $s = 0.25$, $\varphi_1 = \infty$, $q_1 = 2$

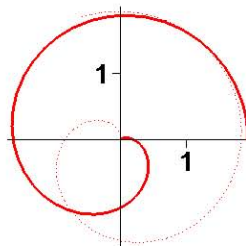
a



b



c



d

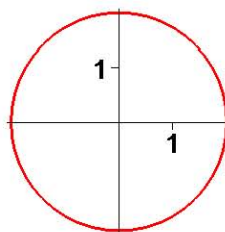


Fig. 7. Terminating orbits in Region II (a-d) and Region II' (e)

(a) $k^2 = 1, e = 1, s = 0.25, \frac{\varphi_2}{\pi} = \infty, q_2 = \infty$

(b) $k^2 = 0.6, e = 1, s = 1.25, \frac{\varphi_2}{\pi} = 0.78496, q_2 = \infty$

(c) $k^2 = 0.5, e = 0.5, s = 0.615920, \frac{\varphi_2}{\pi} = 1.1315, q_2 = 3$

(d) $k^2 = 0.3, e = 0, s = 0.901890, \frac{\varphi_2}{\pi} = 0.78606, q_2 = 1.1805$

(e) $k^2 = 0.095385, e = 0, s = 10, \frac{\varphi_2}{\pi} = 0.13684, q_2 = 0.03267$

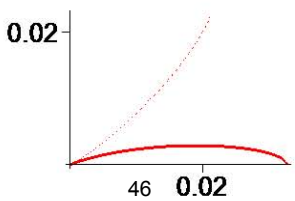
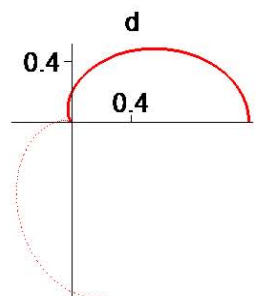
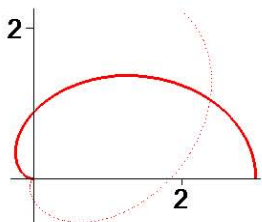
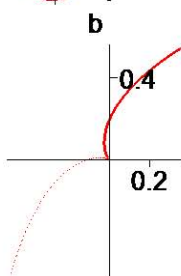
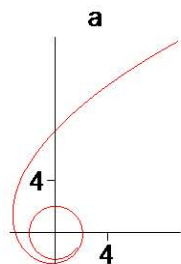


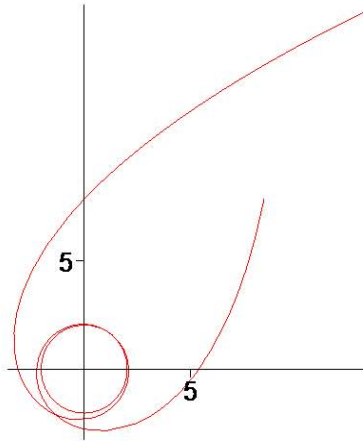
Fig. 8. Unbounded orbits for

(a) $k^2 = 0.99$, $e = 1$, $s = 0.2499968435$, $\frac{\Delta\varphi}{\pi} = 4.6378$

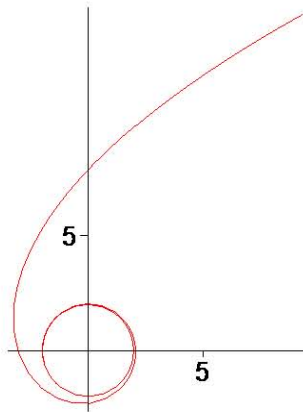
(b) $k^2 = 1$, $e = 1$, $s = 0.25$, $\frac{\Delta\varphi}{\pi} = \infty$

(c) $k^2 = 0.9998000799$, $e = 1$, $s = 0.2501$, $\frac{\varphi_2}{\pi} = 5.0816$

a



b



c

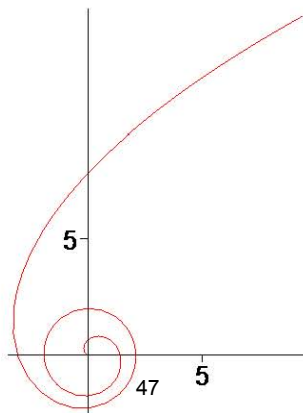


Fig. 9. Trajectories of light for

(a) $U_1 = 0.42922, \Delta\varphi = \pi/2$

(b) $U_1 = 0.56808, \Delta\varphi = \pi$

(c) $U_1 = 0.62334, \Delta\varphi = 3\pi/2$

(d) $U_1 = 0.64720, \Delta\varphi = 2\pi$

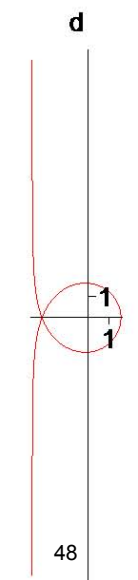
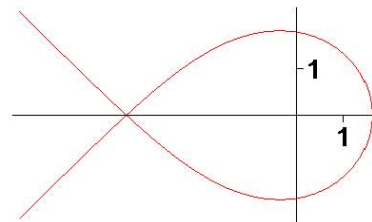
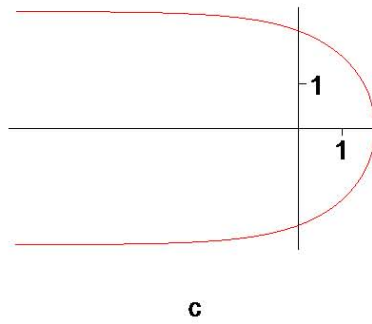
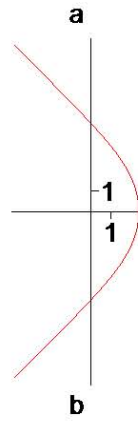


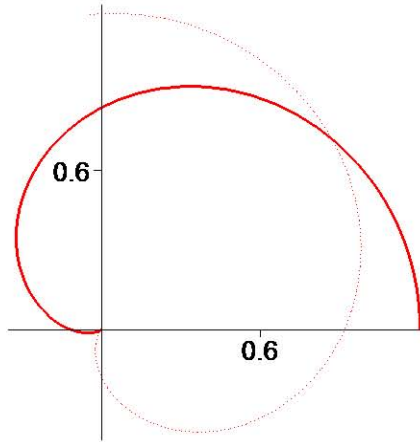
Fig. 10. Trajectories of light that terminated

(a) $U_1 = 0.8333$, $\varphi_1 = 3.8345$

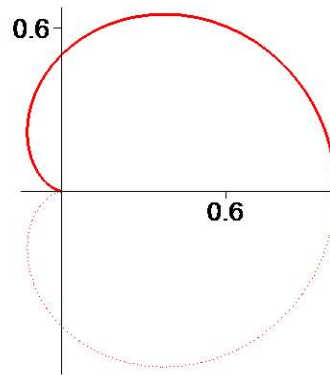
(b) $U_1 = 1$, $\varphi_1 = \pi$

(c) $U_1 = 10$, $\varphi_1 = 0.78133$

a



b



c

